NACA RM L51L04

# RESEARCH MEMORANDUM

## WIND-TUNNEL INVESTIGATION AT HIGH AND LOW SUBSONIC MACH NUMBERS OF A THIN SWEPTBACK WING HAVING AN AIRFOIL SECTION DESIGNED FOR HIGH MAXIMUM LIFT

By Stanley F. Racisz and Nicholas J. Paradiso

Langley Aeronautical Laboratory
Langley Field, Va.

NATIONAL ADVISORY COMMITTEE
FOR AERONAUTICS

WASHINGTON
February 26, 1952

NATIONAL ADVISORY COMMITTEE FOR AERONAUTICS

RESEARCH MEMORANDUM

# WIND-TUNNEL INVESTIGATION AT HIGH AND LOW SUBSONIC MACH NUMBERS OF A THIN SWEPTBACK WING HAVING AN AIRFOIL SECTION DESIGNED FOR HIGH MAXIMUM LIFT

By Stanley F. Racisz and Nicholas J. Paradiso

## SUMMARY

An investigation has been made in the Langley low-turbulence pressure tunnel to determine the lift, drag, and pitching-moment characteristics of a 45° sweptback wing utilizing a new 6-percent-thick symmetrical airfoil section, designated NACA 2-006, designed for high maximum lift at low speeds. The semispan wing had an aspect ratio of 4, taper ratio of 0.6, and the NACA 2-006 airfoil section parallel to the plane of symmetry. The effects on the aerodynamic characteristics of varying the Reynolds number from $2.0 \times 10^6$ to $9.0 \times 10^6$ and of fixed transition were determined at low Mach numbers for the wing with and without a split flap. The wing aerodynamic characteristics were determined for Mach numbers as high as 0.95 at several values of the Reynolds number extending from $1.2 \times 10^6$ to $8.0 \times 10^6$.

A comparison of the aerodynamic characteristics with those obtained for a wing of the same plan form with the NACA 65A006 airfoil section indicated the general conclusion that substantial improvements in the characteristics of the wing were obtained at low speeds by the use of the new airfoil section without compromising the high-speed characteristics, at least within the Mach number range investigated. Definite recommendations regarding the use of the new airfoil section on the wings of transonic aircraft cannot be made, however, until data are obtained in the Mach number range extending above 0.95.

## INTRODUCTION

The use of thin, swept wings not only has resulted in undesirably low maximum lift coefficients at the low speeds corresponding to the landing condition, but also may restrict the practical operating range of lift coefficient to values considerably lower than the maximum because

of unstable breaks in the pitching-moment characteristics (reference 1). In an attempt to obtain high maximum lift coefficients with thin airfoil sections, an analysis of available airfoil data was made by Loftin and Von Doenhoff and an approximate relation between the airfoil pressure distribution and the low-speed maximum lift coefficient was found (reference 2). With the use of that relation, several thin airfoil sections having pressure distributions favorable for high maximum lift at low speeds were derived. A complete discussion of the methods used in the derivation of the airfoil sections and test data at high and low subsonic Mach numbers for two of the derived airfoil sections is given in reference 2. As reported in reference 2, maximum section lift coefficients of the order of 1.3 were obtained for the two symmetrical airfoil sections with a thickness ratio of 0.06 at low subsonic Mach numbers.

Inasmuch as the aerodynamic characteristics of swept wings cannot generally be predicted with sufficient accuracy from airfoil-section data, an investigation has been made in the Langley low-turbulence pressure tunnel of a $45^{\circ}$ sweptback wing of aspect ratio 4 and taper ratio 0.6 with one of the new airfoil sections of reference 2 (NACA 2-006) laid out parallel to the plane of symmetry. This wing plan form was selected because of the availability of data for comparison and is designated 45-4-0.6 in reference 1.

Tests at free-stream Mach numbers below 0.17 were made to determine the effects of varying the Reynolds number from $2.0 \times 10^6$ to $9.0 \times 10^6$ on the aerodynamic characteristics of the wing with and without a split flap and to determine the effect of transition position. The compressibility effects on the wing lift, drag, and pitching-moment characteristics were investigated for free-stream Mach numbers ranging up to 0.95 for several values of the Reynolds number. Measurements were also made of the wing-root bending moment to determine the spanwise center of pressure.

## SYMBOLS

$C_L$ lift coefficient $\left(\frac{2 \times \text{Model lift}}{qS}\right)$

$C_{L_{max}}$ maximum lift coefficient

$C_{L_s}$ highest lift coefficient reached before unstable break in pitching-moment curve

$C_D$ drag coefficient $\left(\frac{2 \times \text{Model drag}}{qS}\right)$

$C_M$ pitching-moment coefficient measured at quarter chord of wing mean aerodynamic chord $\left(\frac{2 \times \text{Model pitching moment}}{qS\bar{c}}\right)$

$C_B$ wing-root bending-moment coefficient $\left(\frac{B}{q\frac{S}{2}\frac{b}{2}}\right)$

B bending moment at wing root, foot-pounds

q free-stream dynamic pressure, pounds per square foot $\left(\frac{1}{2}\rho V_o^2\right)$

$\rho$ free-stream mass density, slugs per cubic foot

$V_o$ free-stream velocity, feet per second

v local velocity, feet per second

S twice model area, 2.778 square feet

b twice model span, feet

$\bar{c}$ mean aerodynamic chord, feet $\left(\frac{2}{S}\int_0^{b/2} c^2\, dy\right)$

y distance along semispan, feet

A aspect ratio of complete wing $(b^2/S)$

c wing chord at any spanwise station, parallel to plane of symmetry, feet

$\alpha$ angle of attack of wing chord line, degrees

R Reynolds number $(\rho V_o \bar{c}/\mu)$

$\mu$ coefficient of viscosity, pound-seconds per square foot

$C_{L_\alpha}$ rate of change of lift coefficient with angle of attack

M free-stream Mach number $(V_o/a_o)$

$a_o$ free-stream speed of sound, feet per second

CP distance from plane of symmetry to center of pressure, fraction of semispan

## APPARATUS AND TESTS

### Apparatus

The investigation was conducted in the 3- by $7\frac{1}{2}$-foot rectangular test section of the low-turbulence pressure tunnel (reference 3). Recent alterations have been made to the tunnel which permit the use of Freon-12 as a test medium. With the use of Freon-12, choking Mach numbers can be obtained in the tunnel test section with the original drive motor and fan. Reynolds numbers as high as $9.75 \times 10^6$ per foot of chord can be obtained at a Mach number of 1.0 and a stagnation pressure of 28 inches of mercury absolute. With the use of air as a test medium at a pressure of 10 atmospheres absolute, Reynolds numbers of the order of $12 \times 10^6$ per foot of chord can be obtained at Mach numbers below 0.2.

For the present investigation, a balance equipped with electrical resistance strain gages was used to measure the lift, drag, pitching moment, and root bending moment of a semispan model. The end of the model extending beyond the plane of symmetry passed through the end plate in the tunnel wall and was attached to the balance as shown in figure 1. A labyrinth-type seal (fig. 1) was used to minimize the effects of leakage through the slot between the model and end plate.

### Model

The semispan wing tested in the investigation was constructed of aluminium alloy and had $45^\circ$ sweepback measured at the quarter-chord line, aspect ratio 4, and taper ratio 0.6. The wing plan form, tip shape, and size were the same as for the wing designated 45-4-0.6 in reference 1. A sketch and a photograph of the model are presented in figures 2 and 3, respectively. Ordinates for the plain airfoil section parallel to the plane of symmetry are given in table 1. In figure 4 the profiles and theoretical pressure distributions at zero lift of the NACA 2-006 airfoil section and an NACA 65A006 airfoil section are compared. Tests were made of the model with aerodynamically smooth surfaces and for three conditions of surface roughness. The three types of surface roughness employed consisted in a $\frac{1}{4}$-inch-wide roughness strip beginning at the 0.05c position, a $\frac{1}{4}$-inch-wide roughness strip beginning at the

0.10c position, and leading-edge roughness. The leading-edge roughness extended over a surface length of 0.08c back from the leading edge on the upper and lower surfaces. For the three types of roughness, carborundum grains of approximately 0.004-inch diameter were spread over a coat of shellac in such a manner as to cover from 5 to 10 percent of the specified area.

In addition to the investigation of the plain wing, tests were made of the model equipped with a $0.5\frac{b}{2}$-span, 0.20c, simulated split flap deflected $60^{\circ}$. The flap was formed from a piece of $\frac{1}{16}$-inch steel bent in the form of a V and extended from the root chord to the midspan (fig. 2).

## Tests

Unpublished low-speed data for the wing designated 45-4-0.6 in reference 1 indicated that for a constant value of the Reynolds number and a small variation of Mach number the aerodynamic characteristics were unaffected by increasing the dynamic pressure from 75 to 400 pounds per square foot. Since the dynamic pressures for most of the tests of the present investigation at both low speeds and high speeds were less than 400 pounds per square foot, the data for most of the test conditions should be free of appreciable aeroelastic effects. Tests were made of the model in the smooth condition with the flap retracted at Reynolds numbers ranging from $2.0 \times 10^6$ to $9.0 \times 10^6$ for free-stream Mach numbers below 0.2. The effects of fixing transition at 0.05c, 0.10c, and the leading edge on the plain wing were determined at a Reynolds number of $3.0 \times 10^6$. The effectiveness of the split flap was investigated for the smooth wing and for the wing with leading-edge roughness for Reynolds numbers from $3.0 \times 10^6$ to $9.0 \times 10^6$.

The high-speed investigation consisted in measurements of the aerodynamic characteristics of the plain, smooth wing for a range of Mach number extending from 0.4 to approximately 0.95 for several values of the stagnation pressure, so as to provide information on the effect of Reynolds number throughout the Mach number range. The lift, drag, pitching moment, and root bending moment were determined from approximately zero lift to beyond the stall for most of the high-speed and low-speed tests.

## Corrections

Two types of corrections are necessary in order to convert data obtained in the tunnel to equivalent free-air data. These corrections result from the presence of the tunnel walls, and in the high-speed tests, from the fact that Freon-12 instead of air was employed as a test medium. The only correction applied to the low-speed data was that necessitated by a tunnel-wall-induced upwash. The method of determining this correction is described in reference 4. In addition to the induced-upwash correction, a small blocking correction (less than 2 percent) was applied to the high-speed data obtained in Freon-12. The methods of reference 5 were used to convert the data obtained in Freon to equivalent air data.

Data obtained near Mach number 1.0 may be subject to effects attributable to tunnel choking. Since the phenomenon of tunnel choking corresponds to no free-air condition, data which are influenced by choking cannot be corrected. Correlation of the wing characteristics with measured pressure distributions along the ceiling of the tunnel provided an indication of the onset of the effect of the choking phenomenon on the wing characteristics. All data presented are believed to be free of the effects of choking.

## Precision of Measurements

The values of lift coefficient, pitching-moment coefficient, and root bending-moment coefficient are estimated to be accurate within 3 percent throughout the range of Mach number and Reynolds number investigated. Measurements of the drag with the balance are estimated to be within 1/2 pound of the actual drag. The estimated range of error in the drag coefficient determined at low speeds extended from 0.005 at a Reynolds number of $2.0 \times 10^6$ to 0.001 at a Reynolds number of $9.0 \times 10^6$. For the high-speed tests in Freon-12, the estimated range of error in drag coefficient extended from 0.001 at a Mach number of 0.87 and a Reynolds number of $8.6 \times 10^6$ to 0.005 at a Mach number of 0.4 and a Reynolds number of $2.8 \times 10^6$.

# RESULTS AND DISCUSSION

The wing of the present investigation will be hereinafter referred to as wing 1 and that of reference 1 with the NACA 65A006 airfoil section will be referred to as wing 2.

## Low-Speed Results

The low-speed aerodynamic characteristics of the plain wing at Reynolds numbers ranging from $2.0 \times 10^6$ to $9.0 \times 10^6$ are presented in figure 5. The effects of fixing transition at 0.05c and 0.10c and of leading-edge roughness on the characteristics of the wing are shown in figure 6 for a Reynolds number of $3.0 \times 10^6$. The characteristics of the wing equipped with a 0.5b/2 simulated split flap deflected 60° are shown in figure 7 for Reynolds numbers from $3.0 \times 10^6$ to $9.0 \times 10^6$.

Lift and pitching moment of wing without flap.- The data for wing 1 presented in figure 5 indicate that variations in Reynolds number between $2.0 \times 10^6$ and $9.0 \times 10^6$ caused no large changes in the type of stall, slope of the lift curve measured near zero lift, and angle of attack for maximum lift. The slope of the lift curve is approximately the same as the theoretical slope obtained from reference 6. Of interest is the fact that the slopes of the lift curves at Reynolds numbers of about $2.0 \times 10^6$ and $3.0 \times 10^6$ show some increases in the range of lift coefficient from 0.4 to 0.8, whereas at Reynolds numbers of $6.0 \times 10^6$ and $9.0 \times 10^6$, the lift curves are essentially linear up to the beginning of the stall. Some indication of the nature of the differences in the lift curves at $2.0 \times 10^6$ and $3.0 \times 10^6$ as compared with those at $6.0 \times 10^6$ and $9.0 \times 10^6$ can be obtained from a study of references 1, 7, and 8. As discussed in reference 1, leading-edge separation on thin swept wings with small leading-edge radii occurs at low angles of attack. Reattachment of the flow causes a "bubble" of separated flow, and within the bubble a strong vortex extending along the span with its core near the leading edge of the wing root is formed. Increasing the angle of attack causes an increase in the size of the region of separated flow and an increase in sweep angle of the vortex core and causes the vortex core near the wing tip to curve back in the stream direction. The investigation of reference 7 indicates that the formation of a leading-edge vortex is often accompanied by an increase in lift-curve slope and a downward dip of the pitching-moment curve. The fact that both of these phenomena are shown by the data of figure 5 for Reynolds numbers of about $2.0 \times 10^6$ and $3.0 \times 10^6$ seems to indicate the presence of a leading-edge vortex. For Reynolds numbers of $6.0 \times 10^6$ and $9.0 \times 10^6$, the increases in lift-curve slope at the higher angles of attack seem, if present at all, barely within the experimental accuracy; however, since the pitching-moment curves still show the characteristic dip, the vortex flow is presumably still present, although to a reduced extent. This scale effect may be compared with that shown in reference 8, where, for an airfoil with more rounded leading edges, the vortex-type flow seemed to disappear completely with increase in Reynolds number.

A comparison of the low-speed data obtained for wing 1 with those obtained for wing 2 at a Reynolds number of $9.0 \times 10^6$ for the condition without flap is presented on the left side of figure 8(a). The primary differences in the lift curves are that the variation of lift coefficient with angle of attack remains linear for a larger range of lift coefficient for wing 1 and that an increase in maximum lift coefficient of about 0.1 is obtained for wing 1 as compared with wing 2. The shapes of the pitching-moment curves shown in figure 8(d) are generally similar for the two wings; however, the lift coefficient corresponding to the unstable break in the pitching-moment curve is increased by about 0.3 by the use of the NACA 2-006 airfoil section. The data presented in figures 8(d) and 8(e) show that, as would be expected, a shift in the spanwise center of pressure (determined from the lift and root bending-moment data in fig. 5) accompanies the pitching-moment break. The fact that the center of pressure shifts inboard at a higher lift coefficient for wing 1 as compared with wing 2 indicates that tip stalling is delayed by the use of the NACA 2-006 airfoil section. An indication of the rapidity of the inboard progression of the stall on wing 1 as compared with that on wing 2 is given by the change in spanwise center-of-pressure position with lift coefficient shown in figure 8(e).

Some of the data of figure 5 are summarized in figure 9(a) to show the effect of Reynolds number on the maximum lift coefficient $C_{L_{max}}$ and on the lift coefficient corresponding to the unstable break in pitching moment $C_{L_s}$. Also shown in figure 9 for comparison are the corresponding data for wing 2 with the same plan form as the wing of the present investigation but equipped with an NACA 65A006 airfoil section. Figure 9(a) shows that the maximum lift coefficients of both wings were relatively insensitive to variations in the Reynolds number between $3.0 \times 10^6$ and $9.0 \times 10^6$, whereas the same change in Reynolds number increased the value of $C_{L_s}$ from 0.81 to about 0.94 for wing 1 and from 0.52 to 0.65 for wing 2. Although the maximum lift coefficient for wing 1 was only about 0.1 higher than that for wing 2, the value of $C_{L_s}$ was from 0.3 to 0.35 higher than that for wing 2 throughout the range of Reynolds number investigated. The increase in the value of $C_{L_s}$ obtainable by the use of the NACA 2-006 airfoil section represents an increase of approximately 46 percent in the range of operational lift coefficient at low speeds. It is interesting to note that the maximum lift coefficient for wing 1 was slightly lower than the maximum section lift coefficient (reference 2), a characteristic of the effects of sweep on thick wings, whereas for wing 2, the maximum lift coefficient was higher than the maximum section lift coefficient, a characteristic of the effects of sweep on thin wings.

Fixed transition at either 0.05c or 0.10c resulted in values of $C_{L_{max}}$ and $C_{L_s}$ that were very nearly the same as those for the wing in the smooth condition (fig. 6). Fixing transition at the leading edge, however, decreased the value of $C_{L_s}$ from 0.81 to 0.60 and the value of $C_{L_{max}}$ from 1.15 to 1.07. The data of figure 6 in comparison with those of reference 1 indicate that the values of $C_{L_s}$ and $C_{L_{max}}$ for wing 1 with leading-edge roughness are essentially the same as the values for wing 2 with leading-edge roughness. The results obtained with transition fixed at 0.05c and 0.10c indicate the very important fact that only the leading-edge portions of wings employing the NACA 2-006 airfoil section need be kept smooth in order to obtain high values of $C_{L_s}$.

Lift and pitching moment of wing with flap.- The effects of the split flap on the lift and pitching-moment characteristics of wing 1 in the smooth condition are indicated by a comparison of figure 7 with figure 5. The main effects of deflecting the flap were a considerable decrease in the angle of attack for zero lift, a decrease in the angle of attack for maximum lift, and an increase of about 0.15 or 0.20 in the value of $C_{L_s}$. The pitching-moment data for the smooth wing indicate that deflecting the flap 60° had little effect on the absolute value of the pitching-moment coefficient and on the slope of the pitching-moment curve for a particular lift coefficient (figs. 5(b) and 7(b)). Changing the spanwise location of the flap, however, might considerably change the pitching-moment coefficient because of the change in flap location with respect to the quarter-chord point of the mean aerodynamic chord. Data from a few exploratory tests at a Reynolds number of $3.0 \times 10^6$ (not presented) indicated that both $C_{L_{max}}$ and $C_{L_s}$ could be increased by only 0.1 by increasing the flap span from 0.5b/2 to as much as 1.00b/2, with resultant pitching-moment coefficients at zero lift of the order of -0.06 for a 0.75b/2 split flap and -0.10 for a full-span flap.

A comparison of the lift and pitching-moment characteristics of wing 1 with those of wing 2 (figs. 8(a) and 8(d)) indicates that, as for the flap-retracted condition, the lift curve for wing 1 remained linear over a larger range of angle of attack, the value of $C_{L_s}$ was about 0.35 higher for wing 1, and the value of $C_{L_{max}}$ was about 0.1 higher for wing 1. The variations of $C_{L_{max}}$ and $C_{L_s}$ with Reynolds number are shown in figure 9(b) for wings 1 and 2. A comparison of the data presented in figure 9(b) with those presented in figure 9(a) indicates that although the flap had little effect on the maximum lift

coefficient of either wing, the values of $C_{L_s}$ for both wings were increased by about 0.15 or 0.20. Other investigations, such as that reported in reference 8, have also shown that the use of a half-span split flap on a swept wing results in only small increases in maximum lift coefficient. Throughout the range of Reynolds number investigated, the value of $C_{L_s}$ for wing 1 with flap deflected was higher than that for wing 2 by about 0.35.

The effect of leading-edge roughness on the aerodynamic characteristics of wing 1 with the split flap is illustrated by the data presented in figure 7. With leading-edge roughness, the value of $C_{L_s}$ was only about 0.1 higher than that obtained for wing 2 from reference 1.

Drag of wing without flap.- The data of figure 5 indicate that variations of the Reynolds number between $2.0 \times 10^6$ and $9.0 \times 10^6$ generally had little effect on the drag at low and moderate lift coefficients. The drag coefficient at higher lift coefficients decreases somewhat with increasing Reynolds number. A comparison of the drag polars obtained for wings 1 and 2 without flaps, shown in figure 8(b) for a Reynolds number of $9.0 \times 10^6$, indicates that for lift coefficients above 0.6 the drag coefficients of wing 1 are considerably lower than those of wing 2 and at a lift coefficient of 0.9 they are as much as 0.16 lower. No comparisons are made for the minimum drag coefficients of wings 1 and 2 because of the insensitivity of the balance to the small drag loads at low drag coefficients. The lift-drag ratio for wing 1 is shown in figure 8(c) as a function of lift coefficient and indicates that the use of the NACA 2-006 airfoil section may result in a maximum lift-drag ratio appreciably higher than that obtainable with the NACA 65A006 airfoil section.

The effects of fixed transition on the drag characteristics of wing 1 are shown by the data presented in figure 6, which indicate that fixing transition at 0.05c and 0.10c had little effect on the minimum drag of wing 1, whereas leading-edge roughness increased the drag coefficient throughout the range of lift coefficient investigated. A comparison of the drag characteristics of wing 1 with data for wing 2 in reference 1 indicates similar drag polars for both wings with leading-edge roughness.

Drag of wing with flap.- A comparison of the data presented in figure 7 with those presented in figure 5 indicates that deflecting the split flap decreased the drag coefficient at high lift coefficients and increased the drag coefficient at low and moderate lift coefficients. With the flap deflected, the drag coefficients of wing 1 were as much as 0.08 to 0.23 lower than those of wing 2 for lift coefficients above

0.9 (fig. 8(b)). The lift-drag ratios for wing 1 with the flap deflected were higher than those for wing 2 throughout the range of lift coefficient investigated (fig. 8(c)).

The data presented in figure 7 indicate that with the flap deflected, the main effect of leading-edge roughness was an increase in drag coefficient at high lift coefficients. A comparison of the drag polars for wings 1 and 2 with flaps deflected and with leading-edge roughness (fig. 10) indicates similar drag characteristics for both wings.

## High-Speed Results

The aerodynamic characteristics of the plain smooth wing for Mach numbers from about 0.4 to 0.95 and for Reynolds numbers between $1.2 \times 10^6$ and $8.6 \times 10^6$ are presented in figure 11. Drag data for a Reynolds number of $1.193 \times 10^6$ and a Mach number of 0.396 (fig. 11(a)) have not been presented because of the insensitivity of the balance to the small drag loads for that condition. The tests were made at constant values of the stagnation pressures so that variations in the Reynolds number occurred simultaneously with variations in the Mach number. As an aid in interpreting the relatively large amount of data contained in figure 11, some of the more important aerodynamic characteristics of the wing were plotted in such a manner as to show the effect of Mach number on these characteristics for various constant values of the Reynolds number. The maximum lift coefficient, the lift coefficient corresponding to the unstable break in pitching-moment curve, the lift-curve slope, the minimum drag coefficient, and the drag coefficient for a lift coefficient of 0.4 were determined for Reynolds numbers of $2 \times 10^6$, $3 \times 10^6$, $5 \times 10^6$, and $7 \times 10^6$ and are shown as functions of Mach number in figure 12.

Lift and pitching moment.- The results shown in figure 12 indicate that the maximum lift coefficient of wing 1 was relatively insensitive to variations in the Reynolds number and decreased from about 1.15 to about 0.95 as the Mach number increased from 0.1 to 0.7. Increasing the Mach number from 0.1 to the maximum investigated decreased the value of $C_{L_s}$ for all the Reynolds numbers investigated, with the largest decrease occurring at the highest Reynolds number. The lift-curve slope increased with Mach number for all the Reynolds numbers investigated, with the largest increase occurring for a Reynolds number of $3.0 \times 10^6$.

A comparison of the effect of Mach number on $C_{L_{max}}$ and $C_{L_s}$ shown in figure 13 for wings 1 and 2 (unpublished data for wing 2 are included in figs. 13 and 14) indicates that the maximum lift coefficient for

wing 1 is about 0.1 higher than that for wing 2 throughout the Mach number range investigated. The value of $C_{L_s}$ for wing 1 is about 0.3 higher than that for wing 2 for Mach numbers up to approximately 0.4. As the Mach number is increased above 0.4, the value of $C_{L_s}$ for wing 1 decreases and it is about the same as that for wing 2 at a Mach number of 0.85. As can be seen from figure 14(a), the differences in the lift curves for wings 1 and 2 at high Mach numbers were similar to those obtained at low speeds (fig. 8(a)).

Drag.- The minimum drag coefficient and the drag coefficient corresponding to a lift coefficient of 0.4 are shown for wing 1 in figure 12 as a function of Mach number for various Reynolds numbers. Although the accuracy of the minimum drag coefficients is somewhat doubtful for Mach numbers less than about 0.5 and Reynolds numbers less than $3.0 \times 10^6$, the dynamic pressures were large enough at the higher Mach numbers so that the minimum drag coefficients are reasonably accurate. The data of figure 12(b) indicate that the minimum drag coefficients increase from about 0.005 to about 0.009 as the Mach number increases from 0.5 to 0.9. The value of the Reynolds number has little effect on the minimum drag; however, increasing the Reynolds number from $2.0 \times 10^6$ to $7.0 \times 10^6$ causes a substantial reduction in the drag at a lift coefficient of 0.4 for Mach numbers of the order of 0.65.

A comparison of the minimum drag coefficients of wing 1 with those of wing 2, presented in figure 13, indicates that the minimum drag coefficient of wing 1 is higher than that of wing 2 in the range of Mach number for which reasonably accurate measurements of the minimum drag could be made. This is substantiated by a similar comparison of section data in reference 2. The drag coefficient of wing 1 at a lift coefficient of 0.4 is seen to be about 0.01 to 0.02 lower than that of wing 2 up to a Mach number of approximately 0.75, after which the drag coefficient of wing 1 increases relative to that of wing 2 and becomes higher than that of wing 2 for Mach numbers from 0.85 to the maximum Mach number investigated. The high-speed drag polars of wings 1 and 2 shown in figure 14(a) for a Mach number of 0.79 indicate that wing 1 has lower drags at high lift coefficients than wing 2. The lift-drag ratio, shown in figure 14(b) for a Mach number of 0.79, appears to be higher for wing 1 than for wing 2 throughout most of the range of lift coefficient.

Spanwise center of pressure.- The spanwise position of the center of pressure for wings 1 and 2 determined from the root bending moment and lift data at a Mach number of 0.79 was nearly the same for both wings except that the inboard progression of the center of pressure was slightly less rapid for wing 1 than for wing 2 (fig. 14(b)).

## CONCLUDING REMARKS

An investigation has been made in the Langley low-turbulence pressure tunnel to determine the lift, drag, and pitching-moment characteristics at Mach numbers up to about 0.95 of a 45° sweptback wing with an aspect ratio of 4.0, taper ratio of 0.6, and a new 6-percent-thick symmetrical airfoil section designed for high maximum lift coefficients at low speeds. A comparison of the results with those obtained for a wing of the same plan form with the NACA 65A006 airfoil section indicated the general conclusion that substantial improvements in the characteristics of the wing were obtained at low speeds by the use of the new airfoil section without compromising the high-speed characteristics, at least within the Mach number range investigated. Definite recommendations regarding the use of the new airfoil section on the wings of transonic aircraft cannot be made, however, until data are obtained in the Mach number range extending above 0.95. Some of the pertinent results of the investigation can be summarized as follows:

1. The maximum lift coefficient $C_{L_{max}}$ of the wing of the present investigation with and without flap was about 0.1 higher than that of the same wing with the NACA 65A006 airfoil section with and without flap, throughout the range of Mach number investigated.

2. For Mach numbers less than 0.5, the lift coefficient corresponding to the unstable break in the curve of pitching-moment coefficient against lift coefficient $C_{L_s}$ was approximately 0.3 higher for the wing of the present investigation in the smooth condition, with and without flap, than that for the same wing with the NACA 65A006 airfoil section, with and without flap. For Mach numbers greater than 0.5, the value of $C_{L_s}$ for the wing of the present investigation decreased and it was about the same as that of the wing with the NACA 65A006 airfoil section at a Mach number of 0.85.

3. Fixed transition at either 0.05 chord or 0.10 chord had little effect on the value of $C_{L_s}$ or $C_{L_{max}}$, whereas fixing transition at the leading edge decreased the values of $C_{L_s}$ and $C_{L_{max}}$ from 0.81 to 0.60 and from 1.15 to 1.07, respectively, at a Reynolds number of $3.0 \times 10^6$.

4. The drag coefficients for the smooth condition at a lift coefficient of 0.4 were from about 0.01 to 0.02 lower than those for the same wing with the NACA 65A006 airfoil section for Mach numbers up to about 0.75.

Langley Aeronautical Laboratory
National Advisory Committee for Aeronautics
Langley Field, Va.

## REFERENCES

1. Cahill, Jones F., and Gottlieb, Stanley M.: Low-Speed Aerodynamic Characteristics of a Series of Swept Wings Having NACA 65A006 Airfoil Sections. NACA RM L50F16, 1950.

2. Loftin, Laurence K., Jr., and Von Doenhoff, Albert E.: Exploratory Investigation at High and Low Subsonic Mach Numbers of Two Experimental 6-Percent-Thick Airfoil Sections Designed to Have High Maximum Lift Coefficients. NACA RM L51F06, 1951.

3. Von Doenhoff, Albert E., and Abbott, Frank T., Jr.: The Langley Two-Dimensional Low-Turbulence Pressure Tunnel. NACA TN 1283, 1947.

4. Katzoff, S., and Hannah, Margery E.: Calculation of Tunnel-Induced Upwash Velocities for Swept and Yawed Wings. NACA TN 1748, 1948.

5. Von Doenhoff, Albert E., and Braslow, Albert L.: Studies of the Use of Freon-12 as a Testing Medium in the Langley Low-Turbulence Pressure Tunnel. NACA RM L51I11, 1951.

6. DeYoung, John: Theoretical Additional Span Loading Characteristics of Wings with Arbitrary Sweep, Aspect Ratio, and Taper Ratio. NACA TN 1491, 1947.

7. Fitzpatrick, James E., and Foster, Gerald V.: Static Longitudinal Aerodynamic Characteristics of a 52° Sweptback Wing of Aspect Ratio 2.88 at Reynolds Numbers from 2,000,000 to 11,000,000. NACA RM L8H25, 1948.

8. Wilson, Herbert A., Jr., and Lovell, J. Calvin: Full-Scale Investigation of the Maximum Lift and Flow Characteristics of an Airplane Having Approximately Triangular Plan Form. NACA RM L6K20, 1947.

TABLE 1

ORDINATES FOR THE NACA 2-006 AIRFOIL SECTION

[Stations and ordinates in percent airfoil chord]

| Upper surface | | Lower surface | |
|---|---|---|---|
| Station | Ordinate | Station | Ordinate |
| 0 | 0 | 0 | 0 |
| .501 | .937 | .501 | -.937 |
| 2.008 | 1.769 | 2.008 | -1.769 |
| 4.541 | 2.413 | 4.541 | -2.413 |
| 8.114 | 2.818 | 8.114 | -2.818 |
| 12.717 | 2.983 | 12.717 | -2.983 |
| 18.292 | 2.962 | 18.292 | -2.962 |
| 24.727 | 2.810 | 24.727 | -2.810 |
| 31.828 | 2.561 | 31.828 | -2.561 |
| 35.000 | 2.442 | 35.000 | -2.442 |
| 40.000 | 2.254 | 40.000 | -2.254 |
| 45.000 | 2.066 | 45.000 | -2.066 |
| 50.000 | 1.878 | 50.000 | -1.878 |
| 55.000 | 1.691 | 55.000 | -1.691 |
| 60.000 | 1.503 | 60.000 | -1.503 |
| 65.000 | 1.315 | 65.000 | -1.315 |
| 70.000 | 1.127 | 70.000 | -1.127 |
| 75.000 | .939 | 75.000 | -.939 |
| 80.000 | .751 | 80.000 | -.751 |
| 85.000 | .564 | 85.000 | -.564 |
| 90.000 | .376 | 90.000 | -.376 |
| 95.000 | .188 | 95.000 | -.188 |
| 100.000 | 0 | 100.000 | 0 |
| L.E. radius: 0.805 percent c | | | |

NACA

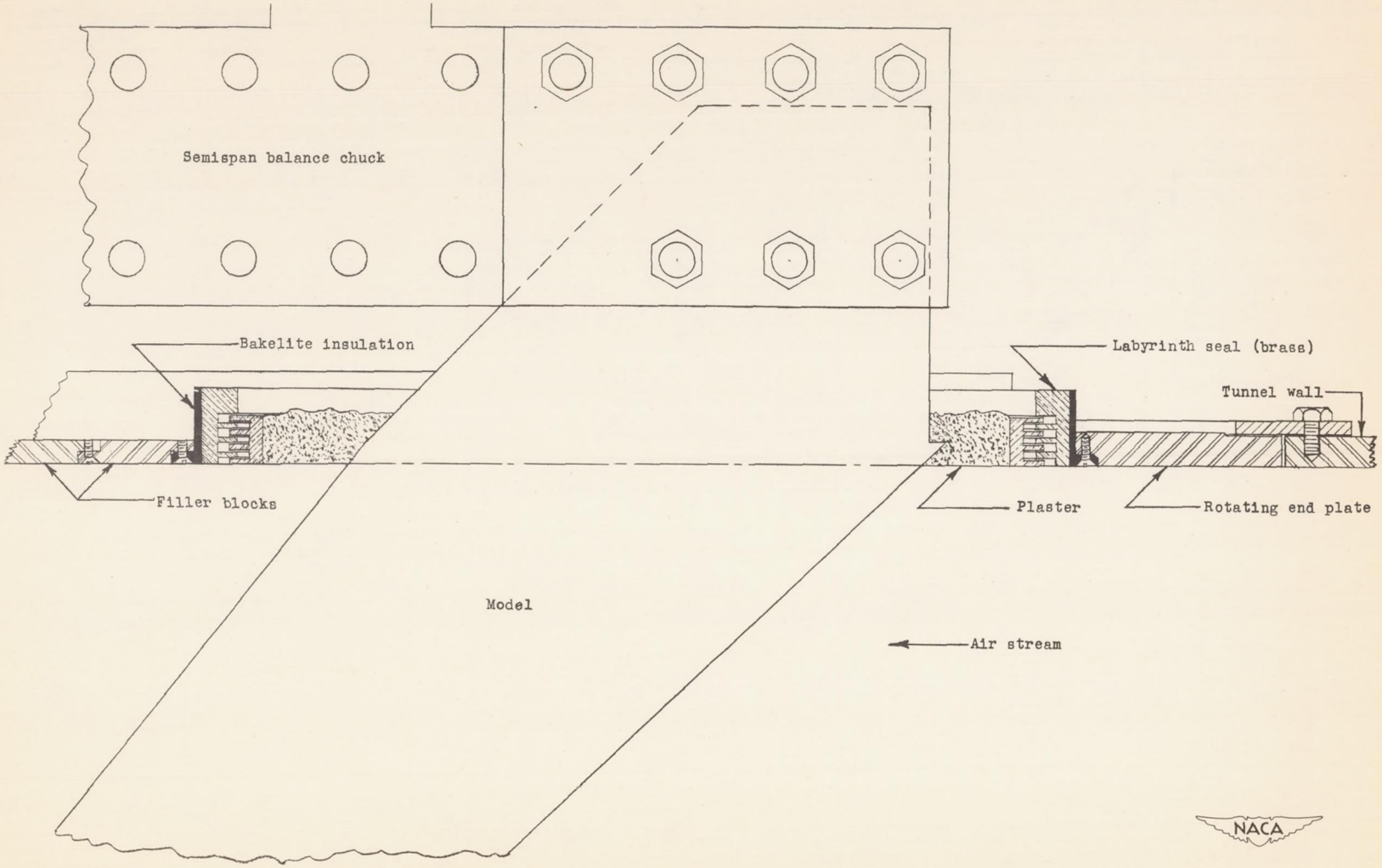


Figure 1.- Method of mounting model on semispan balance.

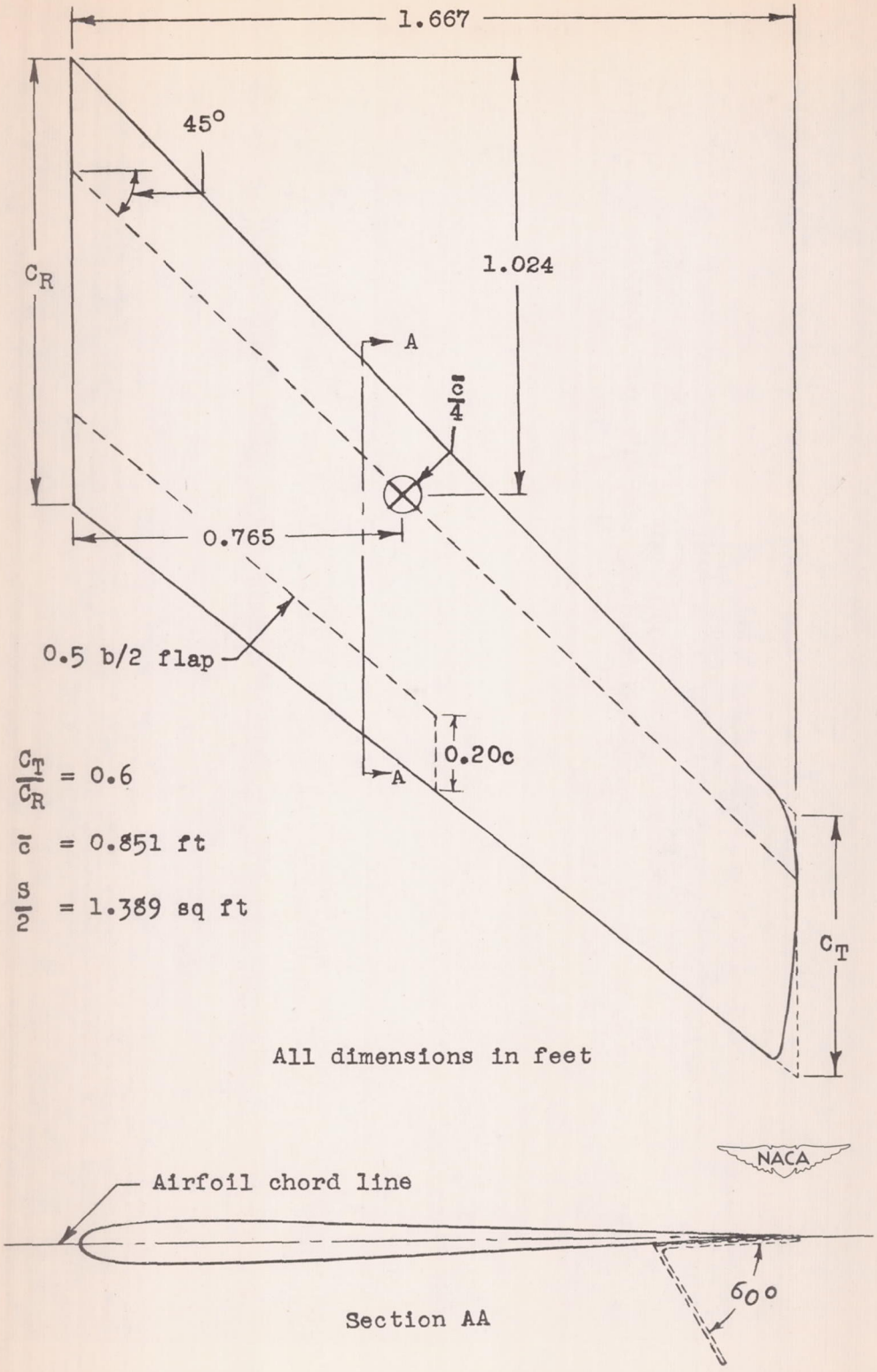


Figure 2.- Sketch of the model with the NACA 2-006 airfoil section.

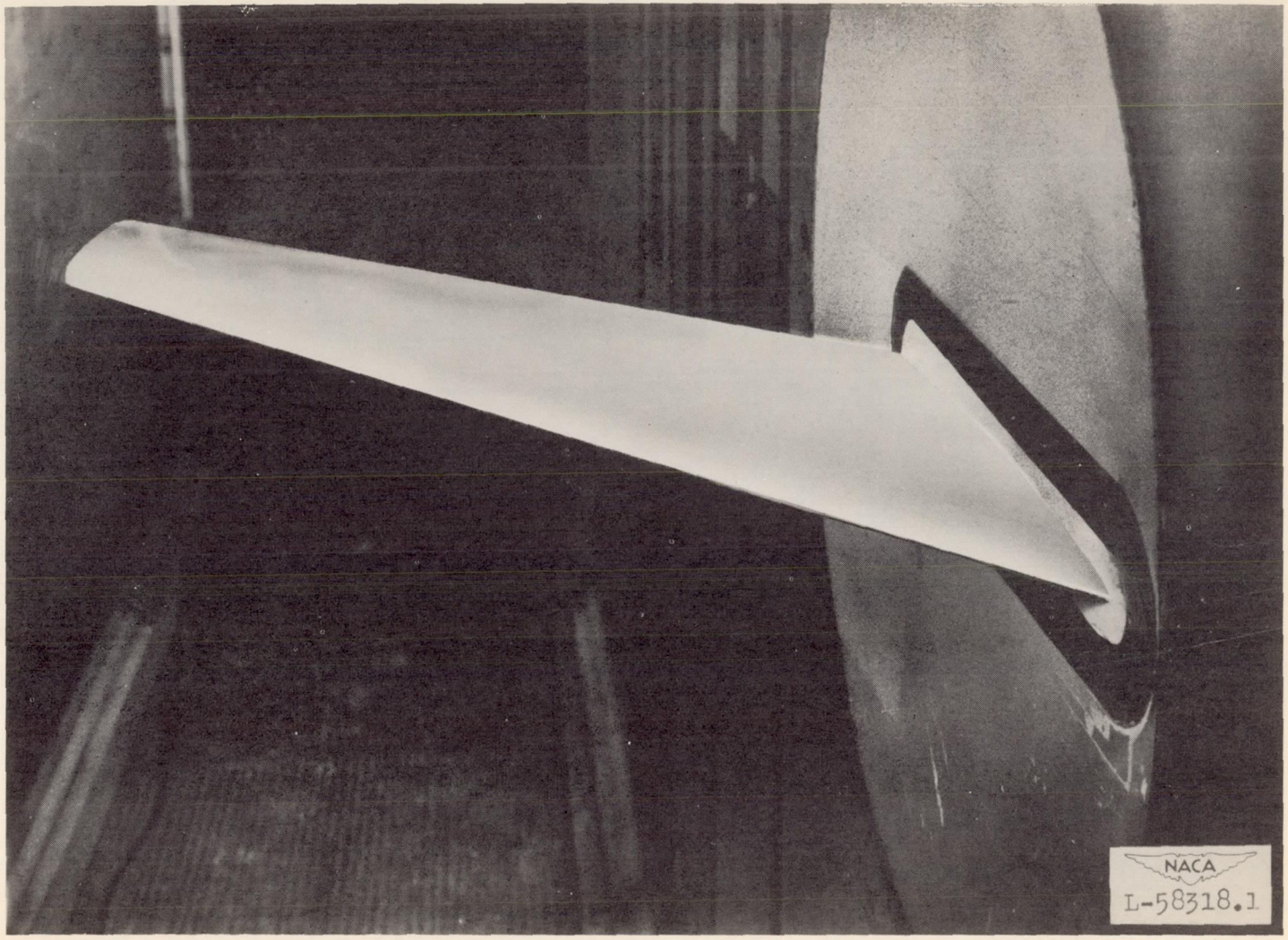


Figure 3.- Photograph of the model in the Langley low-turbulence pressure tunnel.

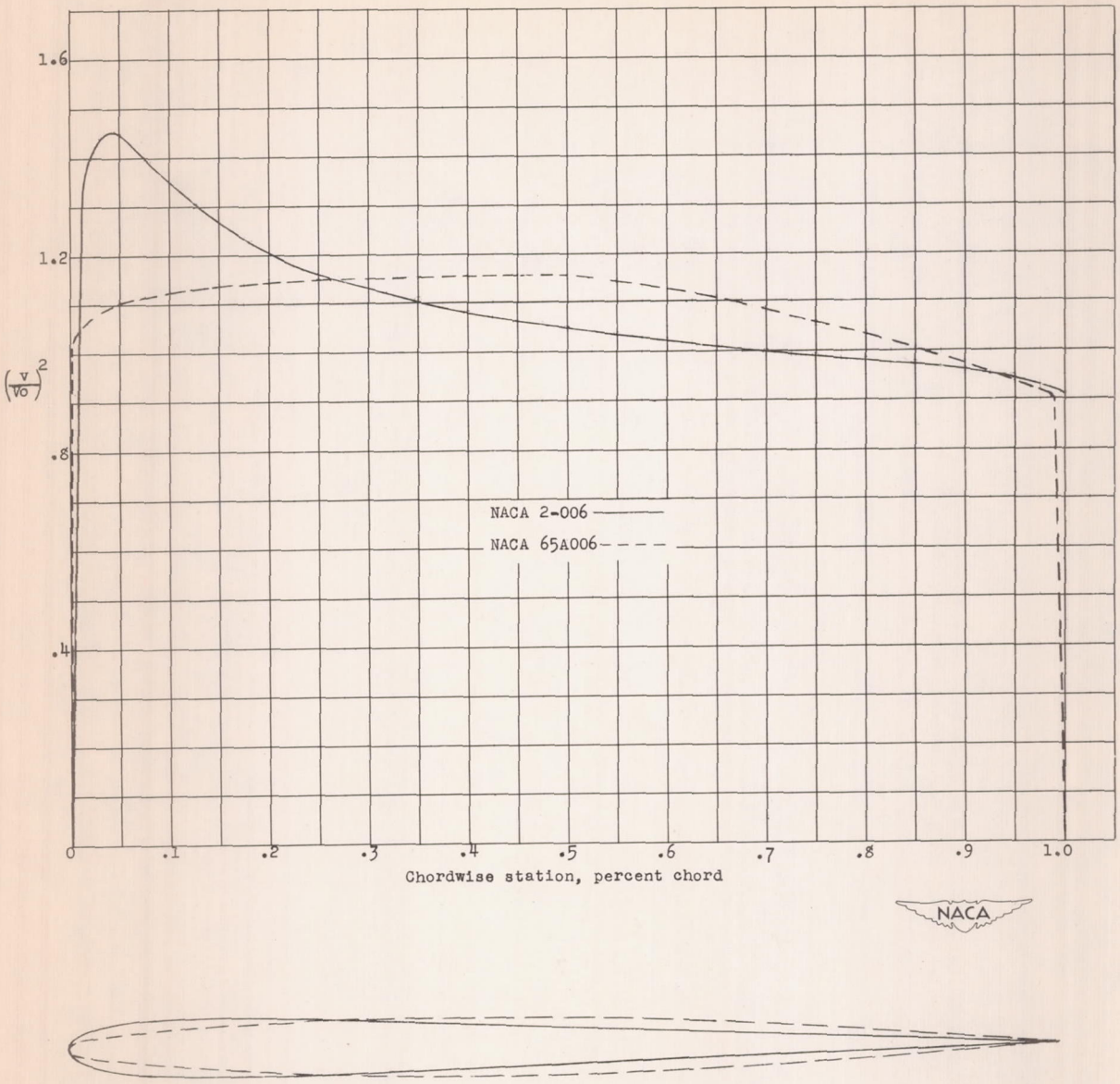


Figure 4.- Theoretical pressure distribution at zero lift and airfoil profiles for the NACA 2-006 and NACA 65A006 airfoil sections.

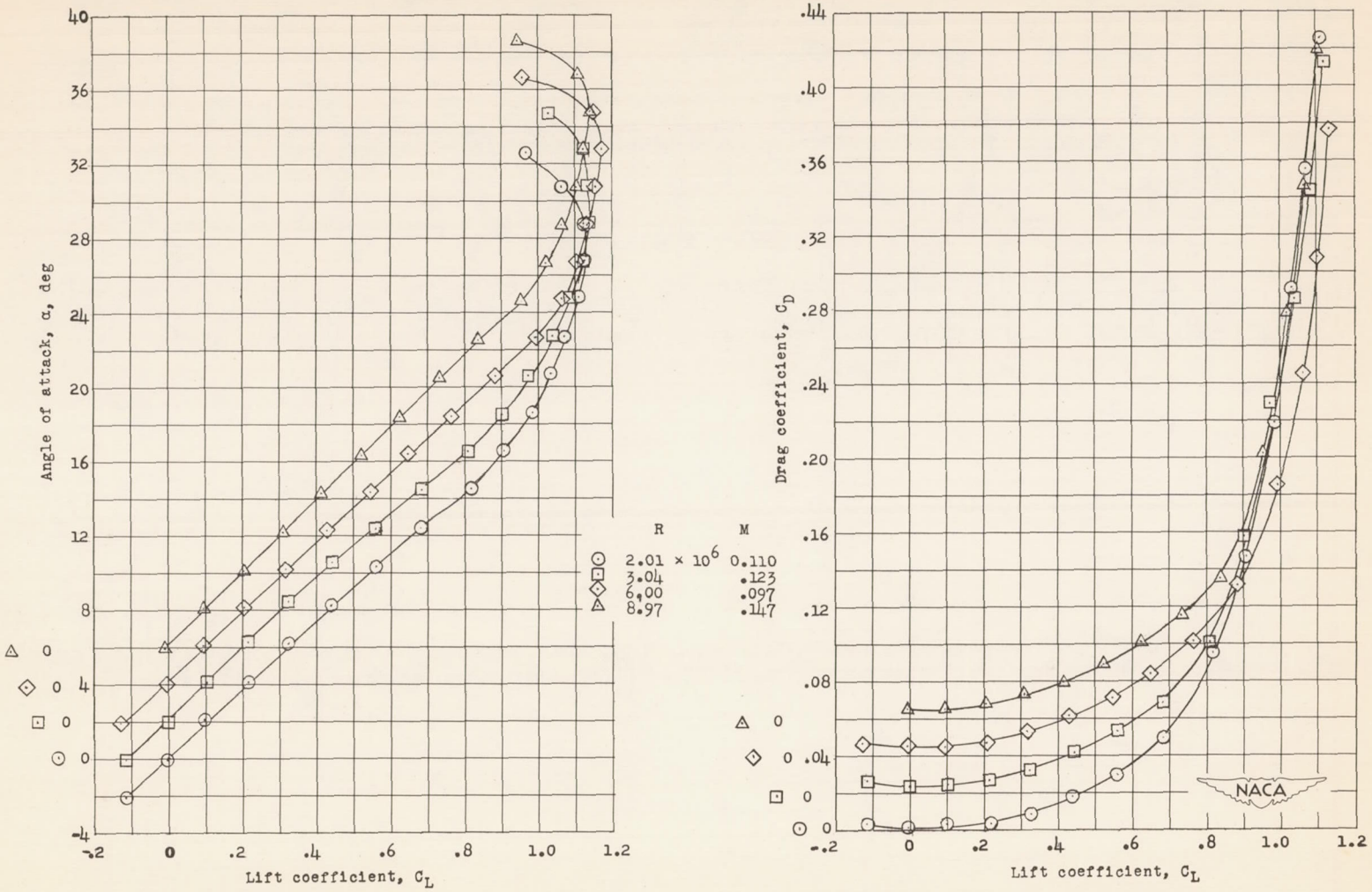


(a) Angle of attack and drag.

Figure 5.- Low-speed aerodynamic characteristics for the plain wing in the smooth condition at various Reynolds numbers. NACA 2-006 airfoil section.

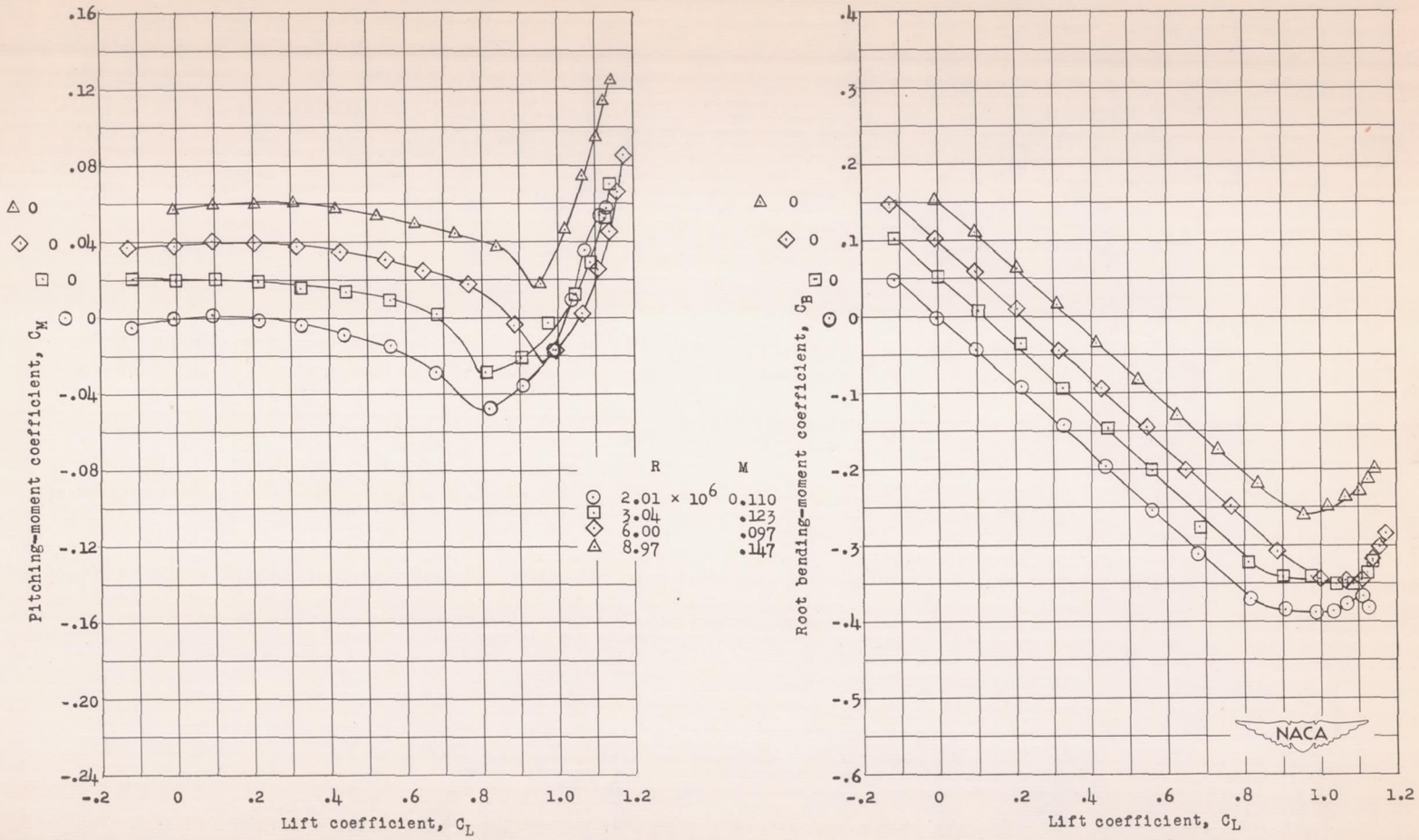


(b) Pitching moment and root bending moment.

Figure 5.- Concluded.

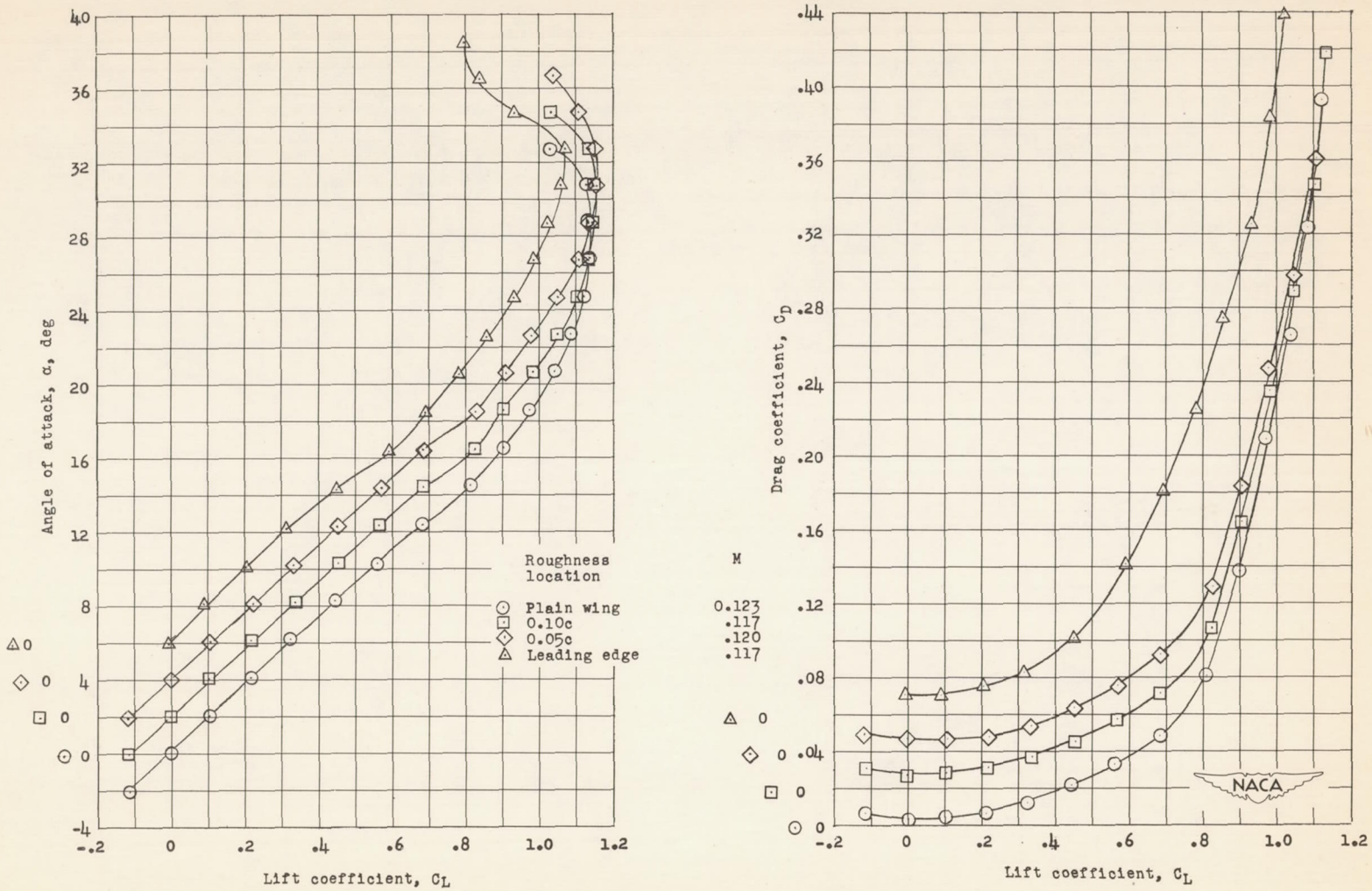


(a) Angle of attack and drag.

Figure 6.- Effect of the transition position on the low-speed aerodynamic characteristics of the wing without a flap. $R = 3 \times 10^6$; NACA 2-006 airfoil section.

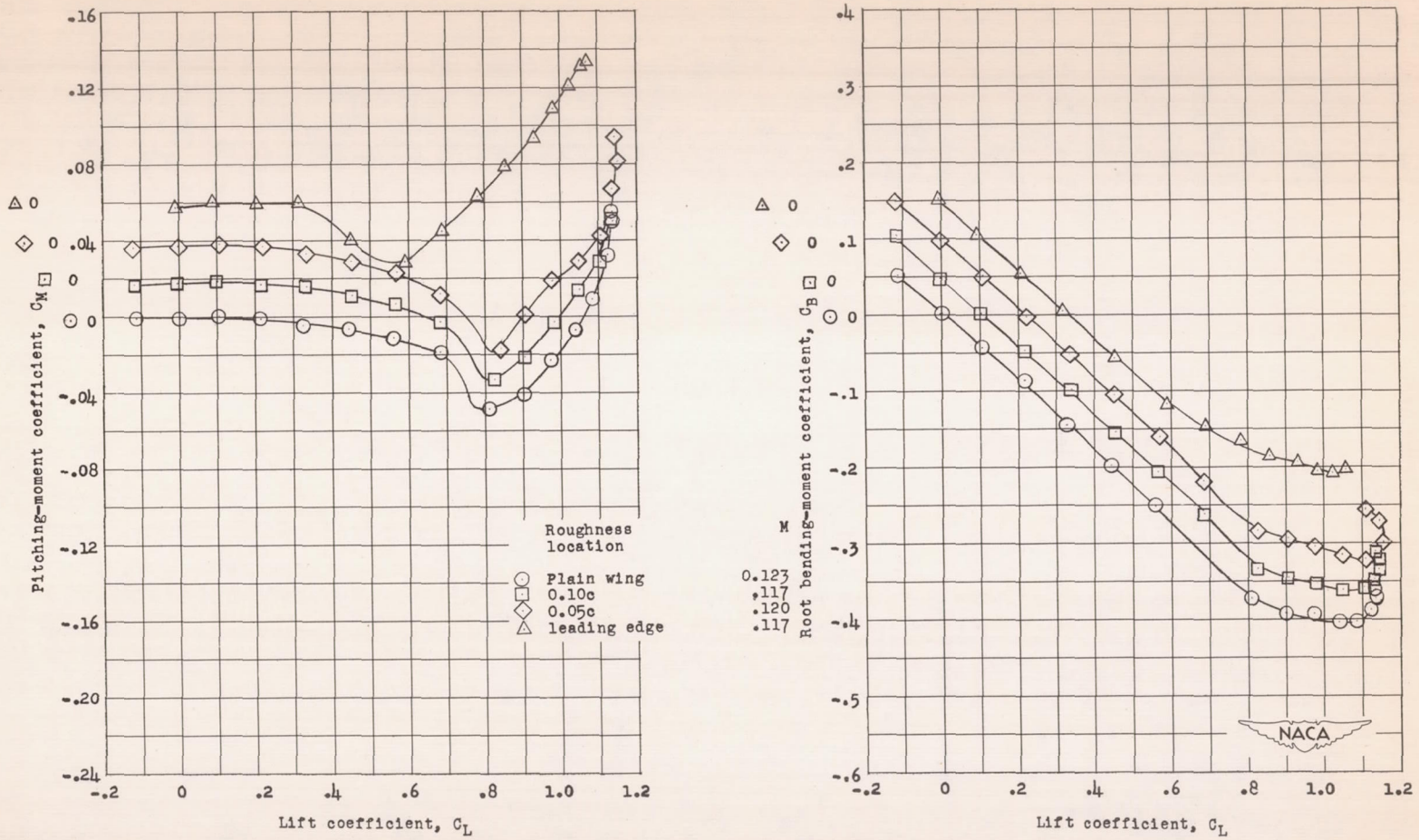


(b) Pitching moment and root bending moment.

Figure 6.- Concluded.

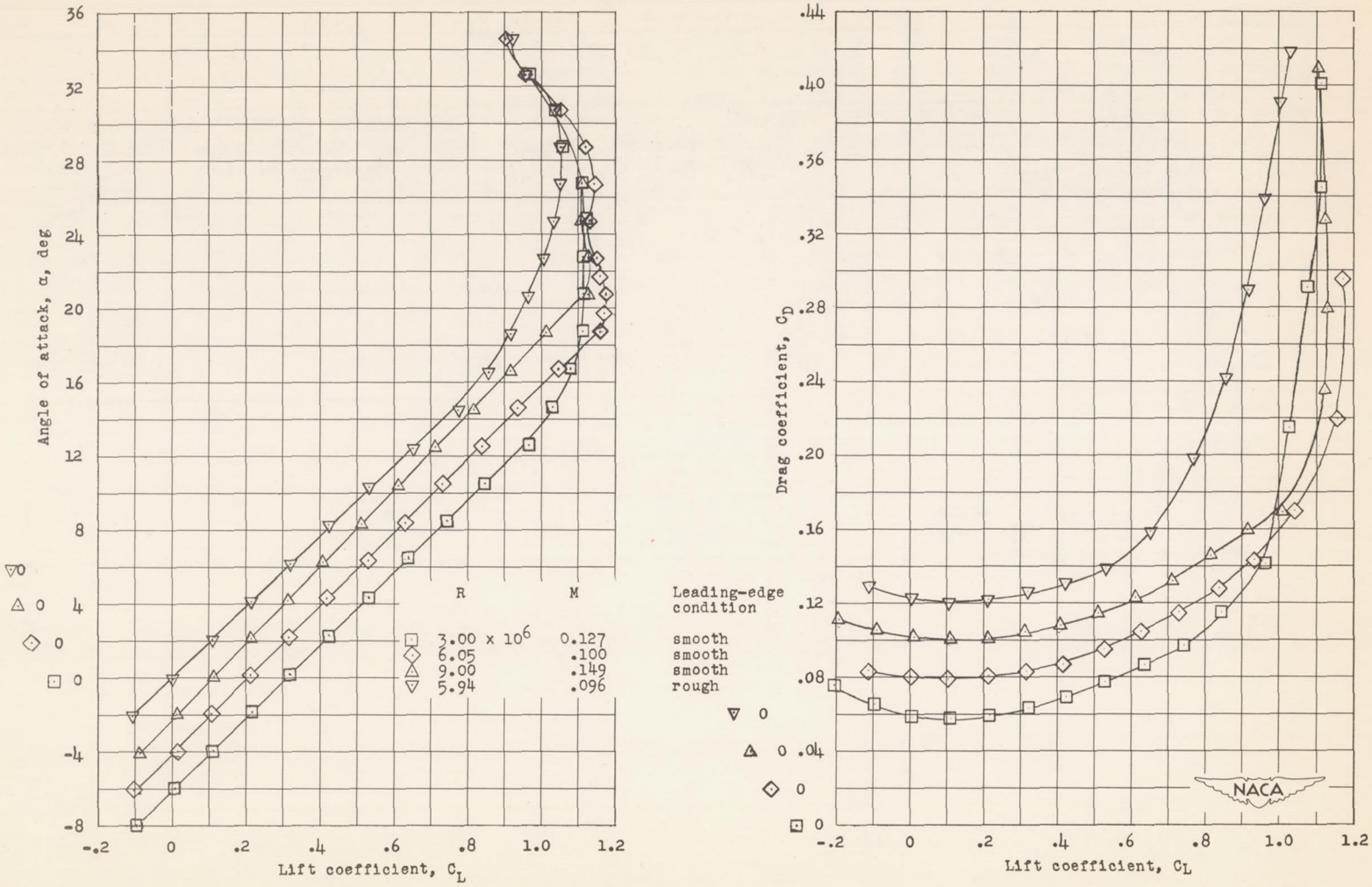


(a) Angle of attack and drag.

Figure 7.- Low-speed aerodynamic characteristics for the wing with a 0.50b/2 split flap deflected 60° for various Reynolds numbers. NACA 2-006 airfoil section.

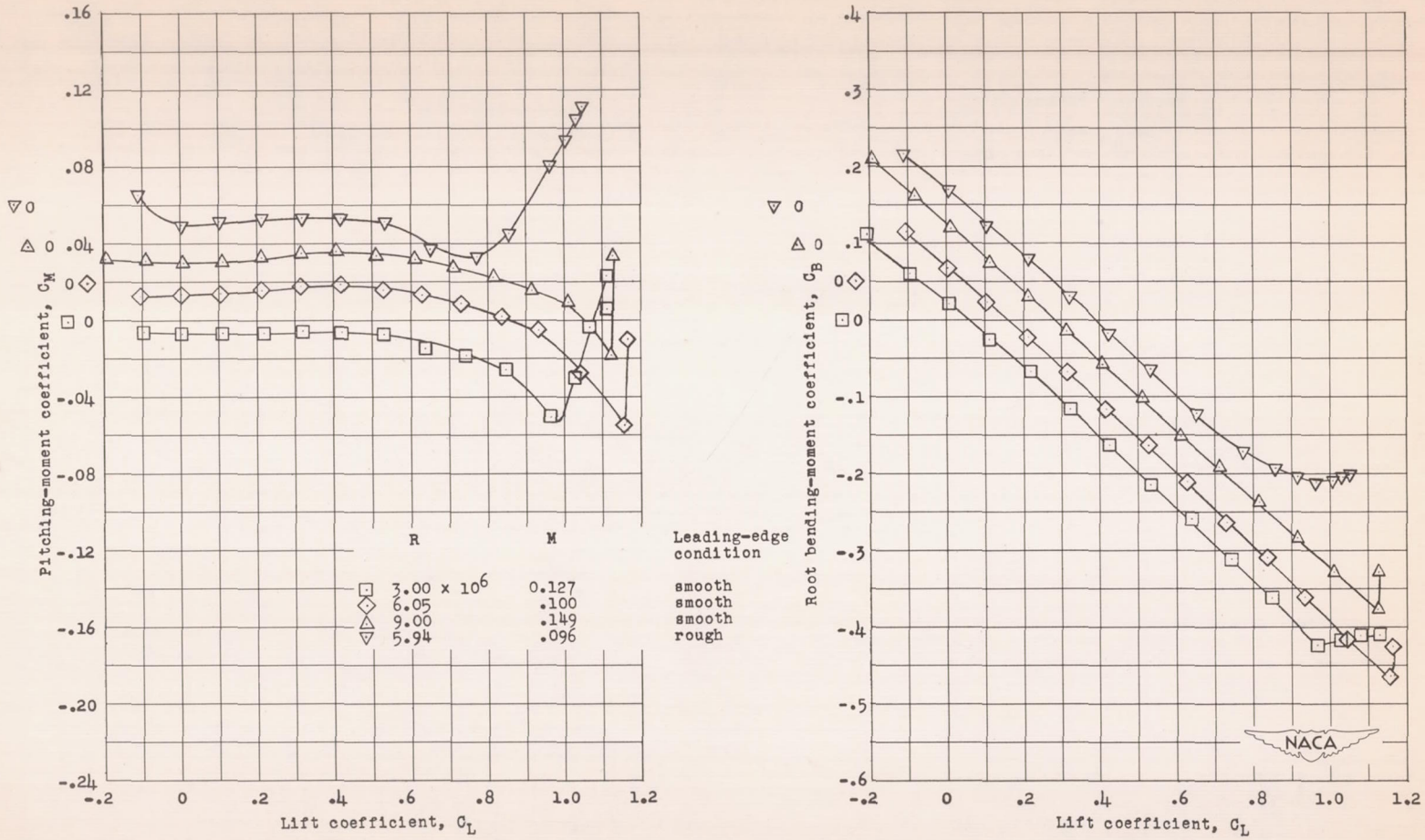


(b) Pitching moment and root bending moment.

Figure 7.- Concluded.

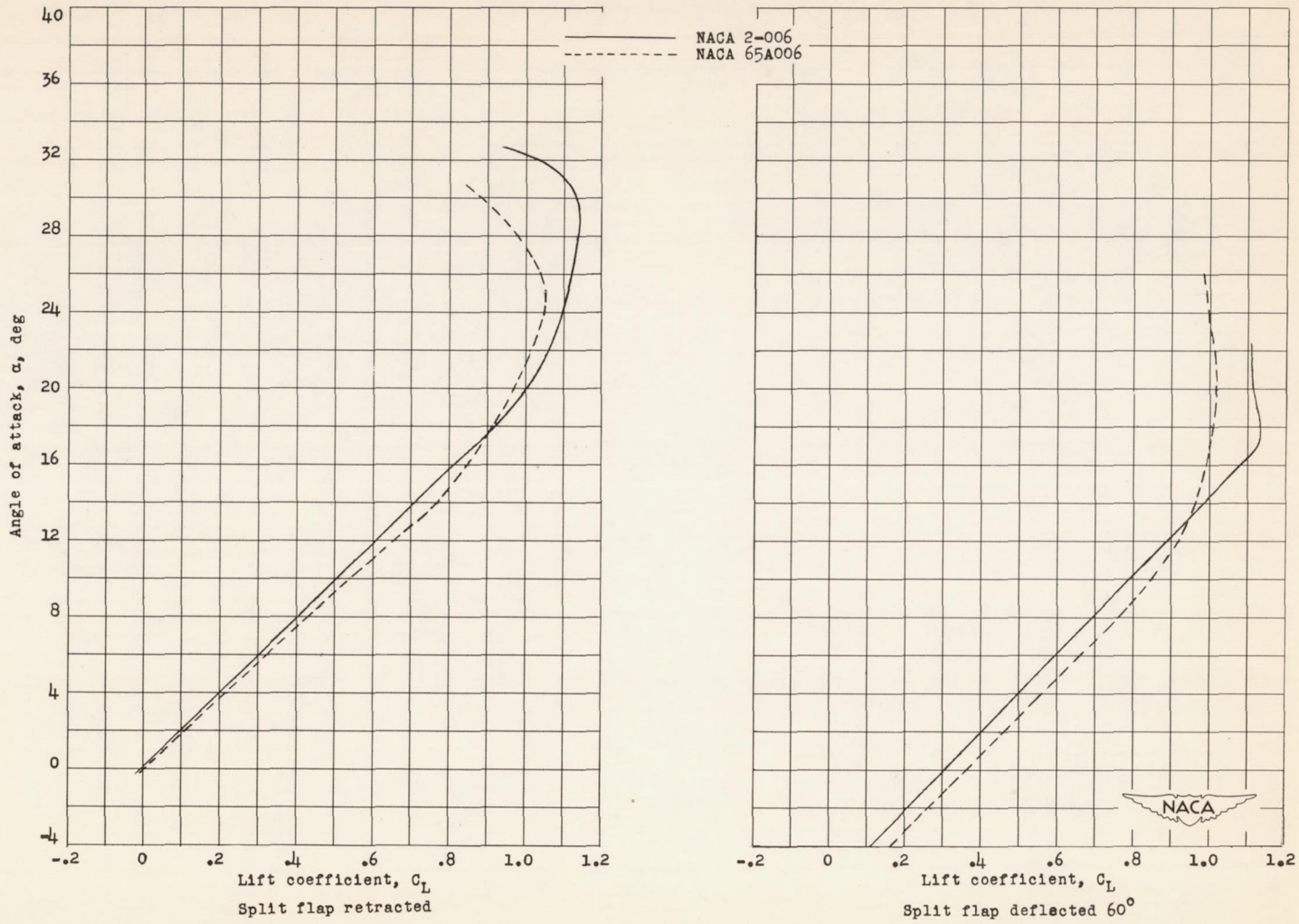


(a) Lift.

Figure 8.- Comparison of the low-speed aerodynamic characteristics of two wings of similar plan form with the NACA 2-006 and NACA 65A006 airfoil sections. Smooth-surface condition; $R = 9 \times 10^6$.

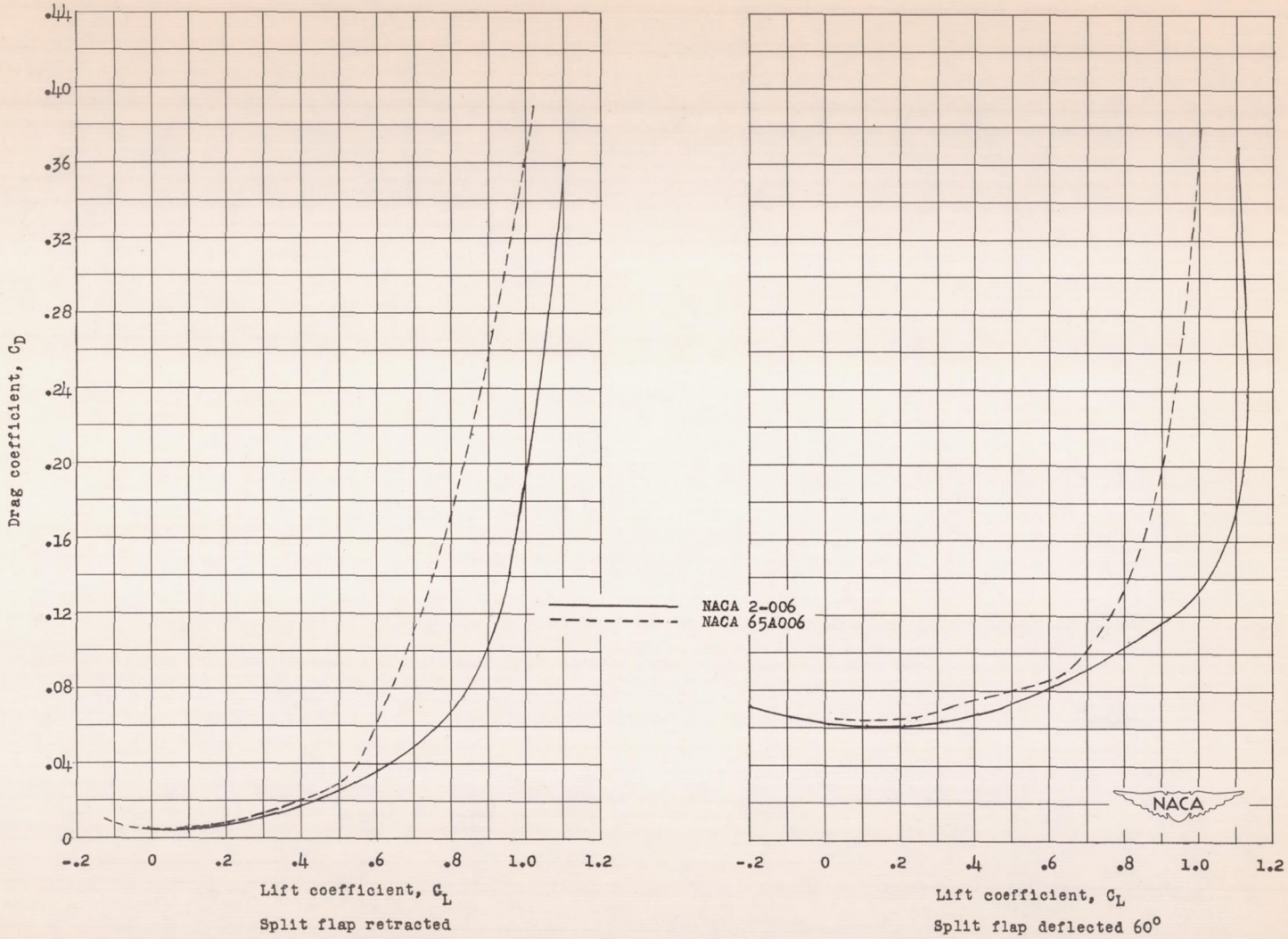


(b) Drag.

Figure 8.- Continued.

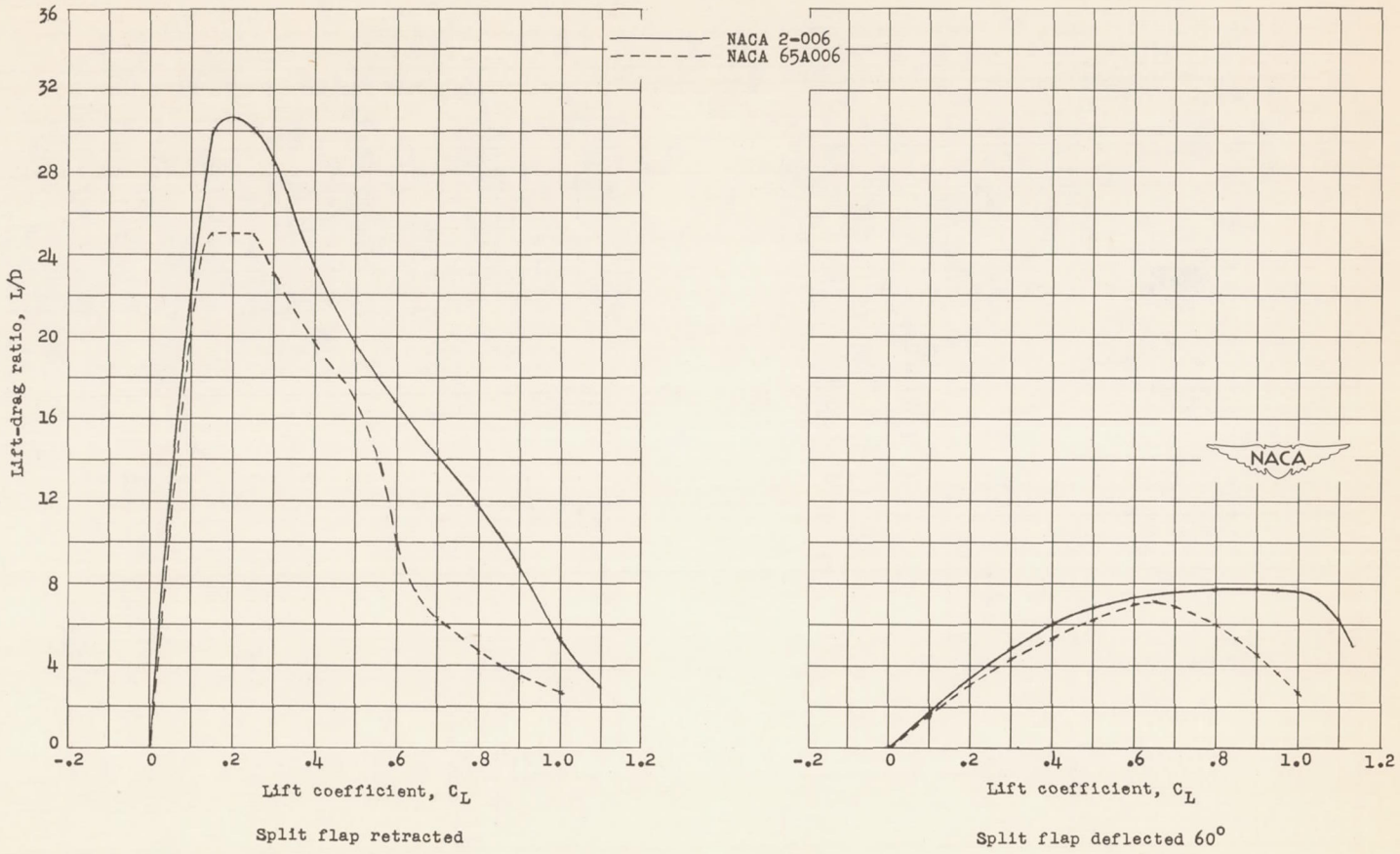


(c) Lift-drag ratio.

Figure 8.- Continued.

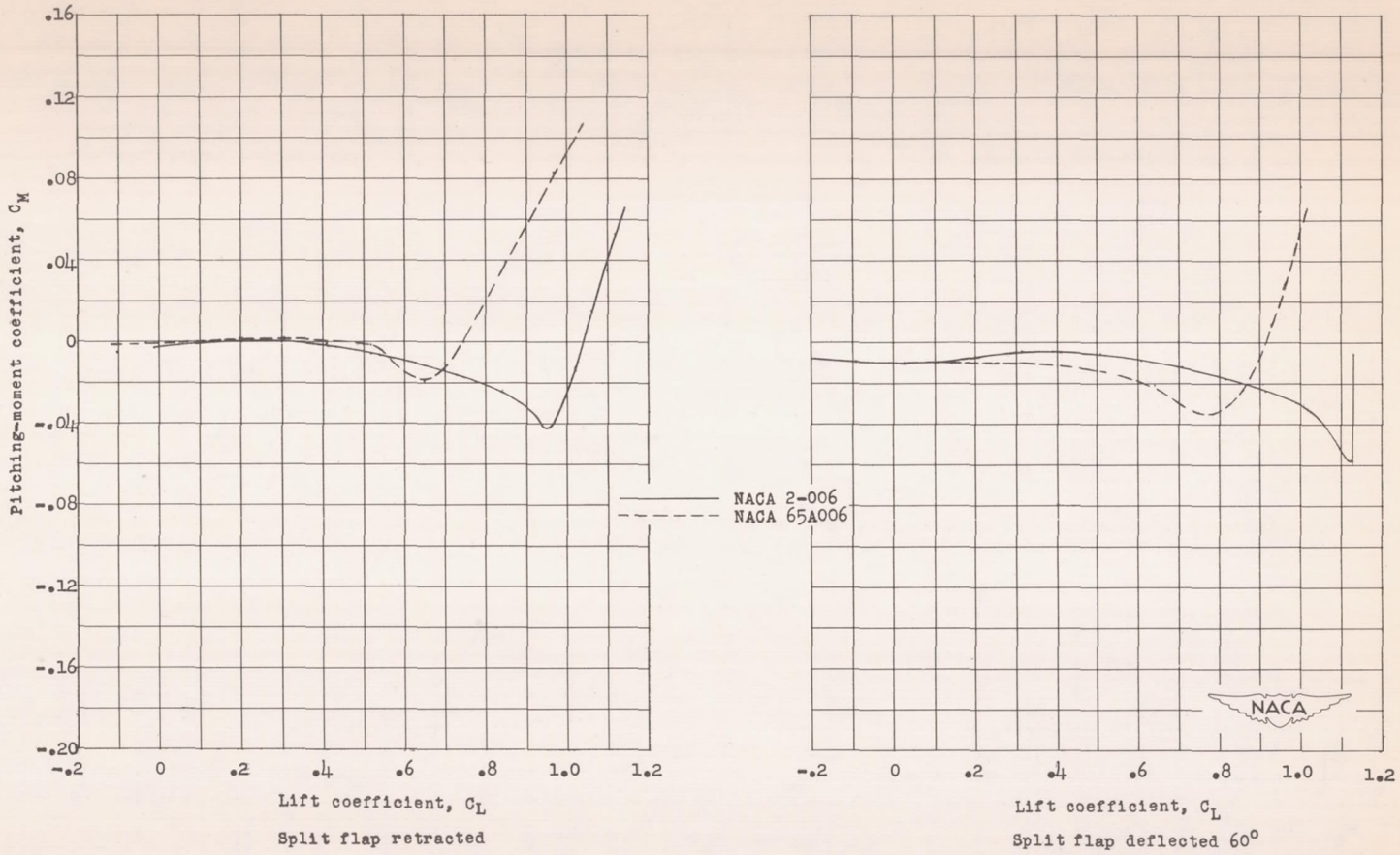


(d) Pitching moment.

Figure 8.- Continued.

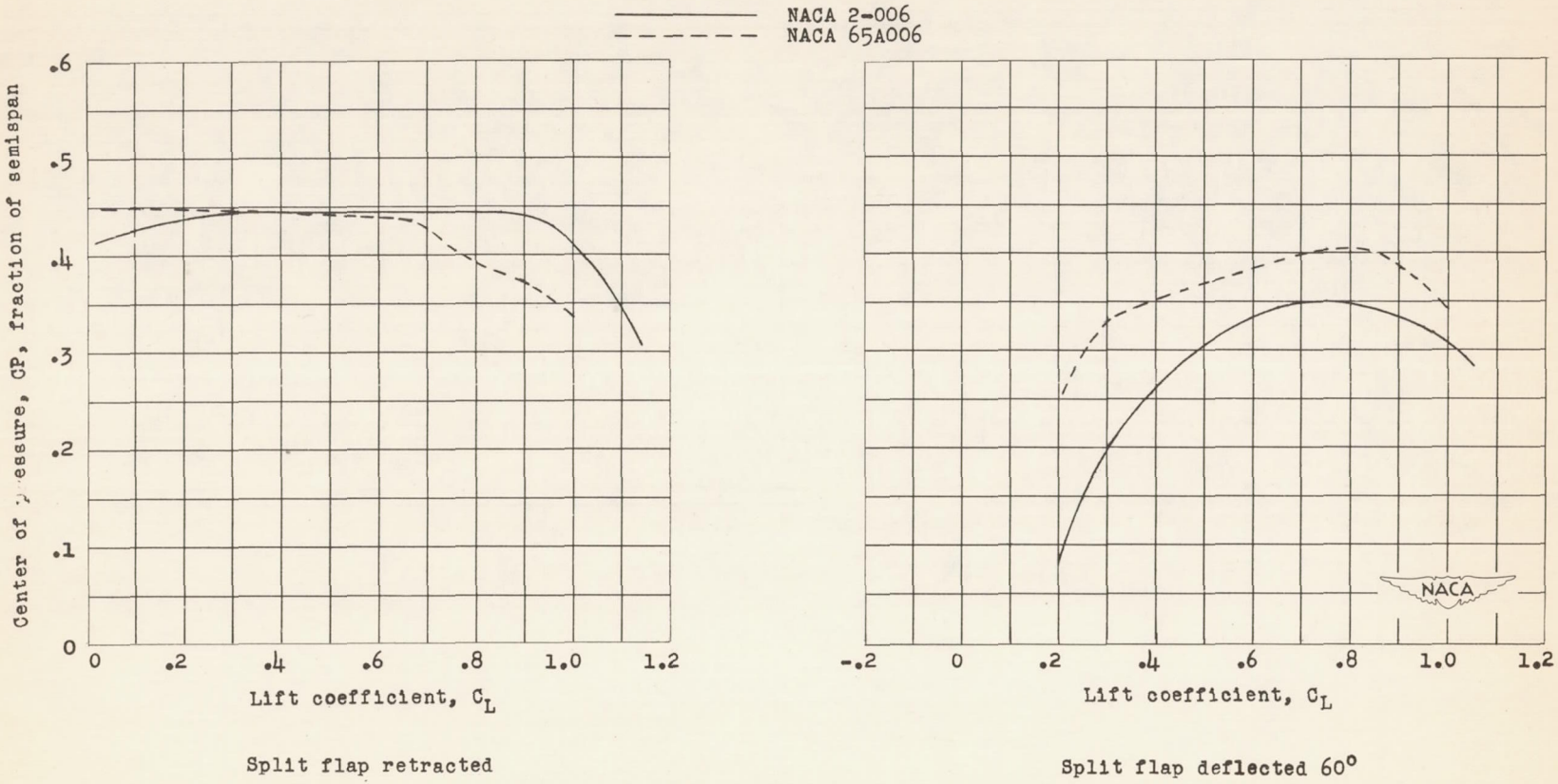


(e) Center of pressure.

Figure 8.- Concluded.

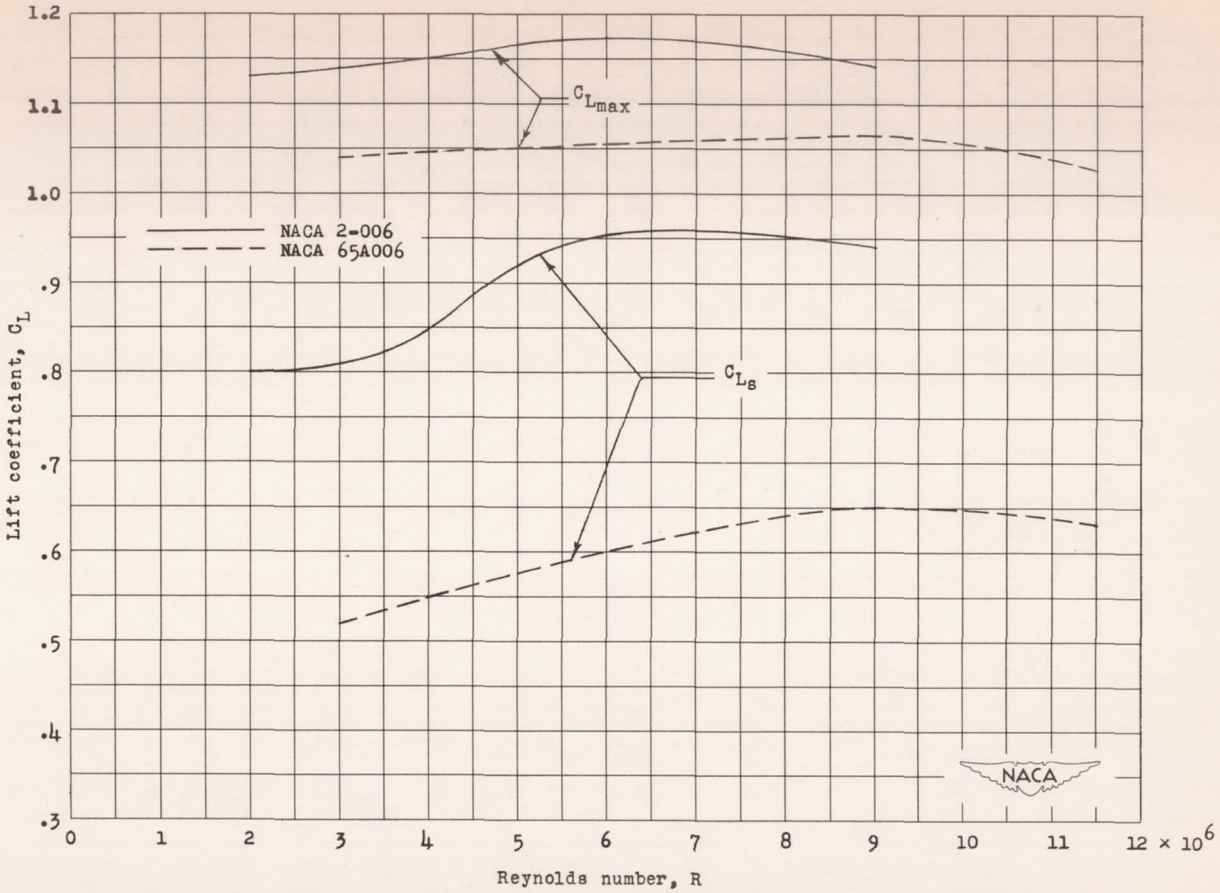


(a) Flap retracted.

Figure 9.- Variation of lift coefficient with Reynolds number for the wing with the NACA 2-006 airfoil section and for the wing with the NACA 65A006 airfoil section.

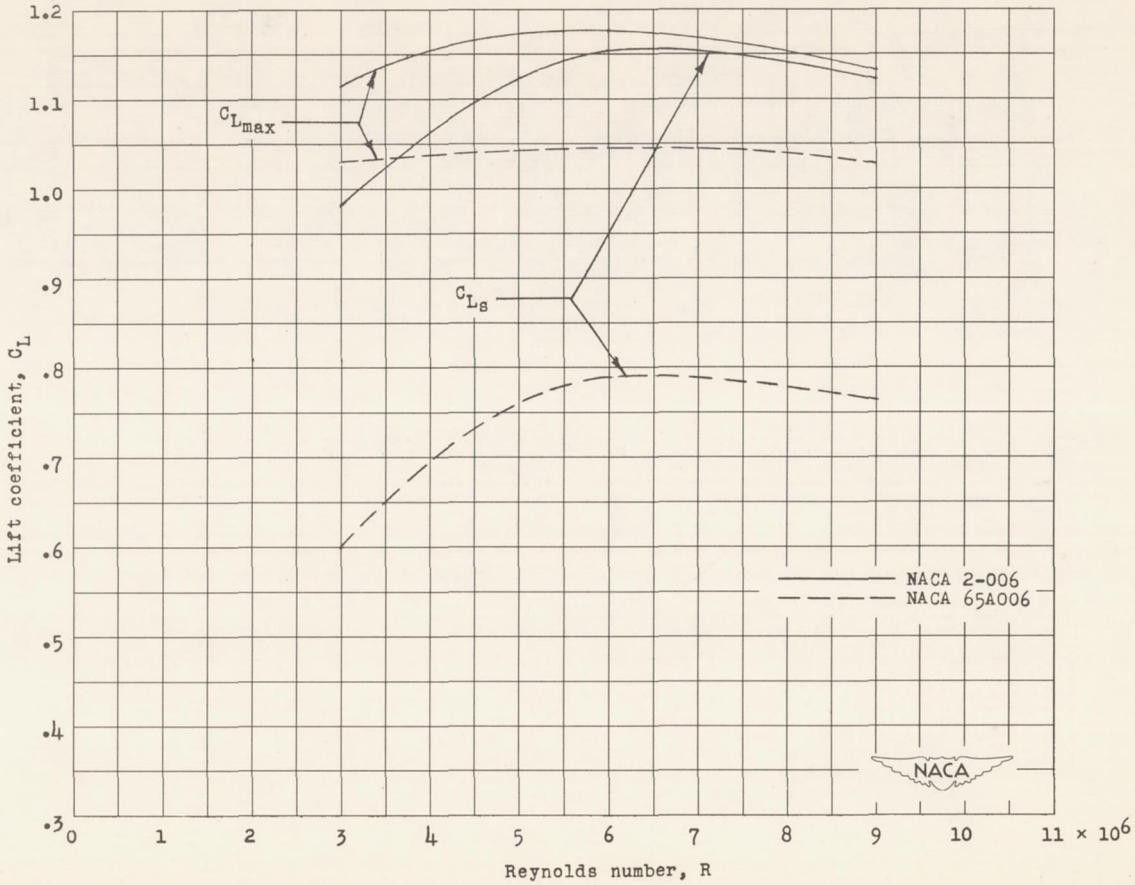


(b) 0.50b/2 flap deflected $60^{\circ}$.

Figure 9.- Concluded.

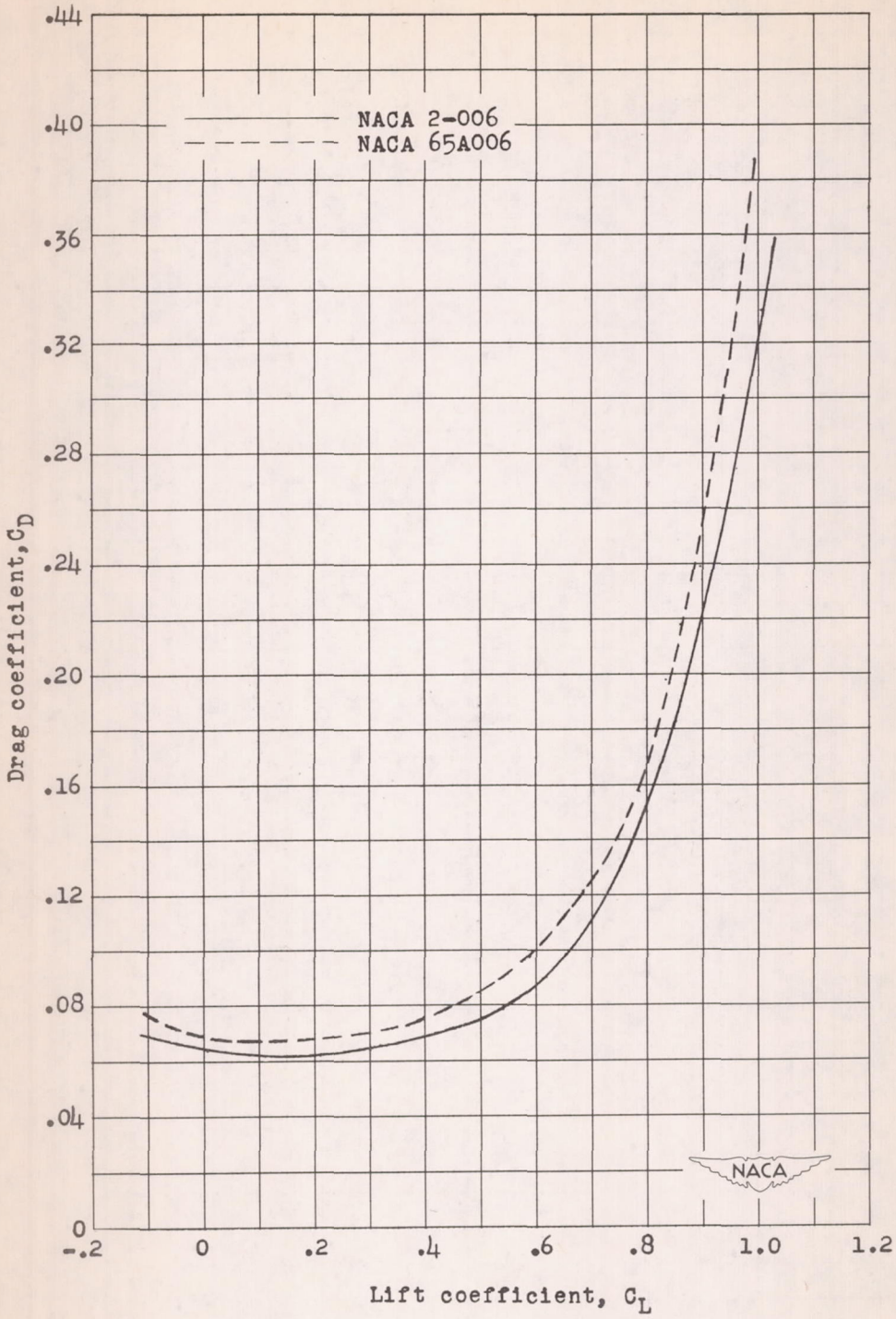


Figure 10.- Comparison of the drag characteristics of two wings of similar plan form with the NACA 2-006 and NACA 65A006 airfoil sections and 0.5b/2 split flaps deflected 60°. Leading-edge roughness; $R = 6 \times 10^6$.

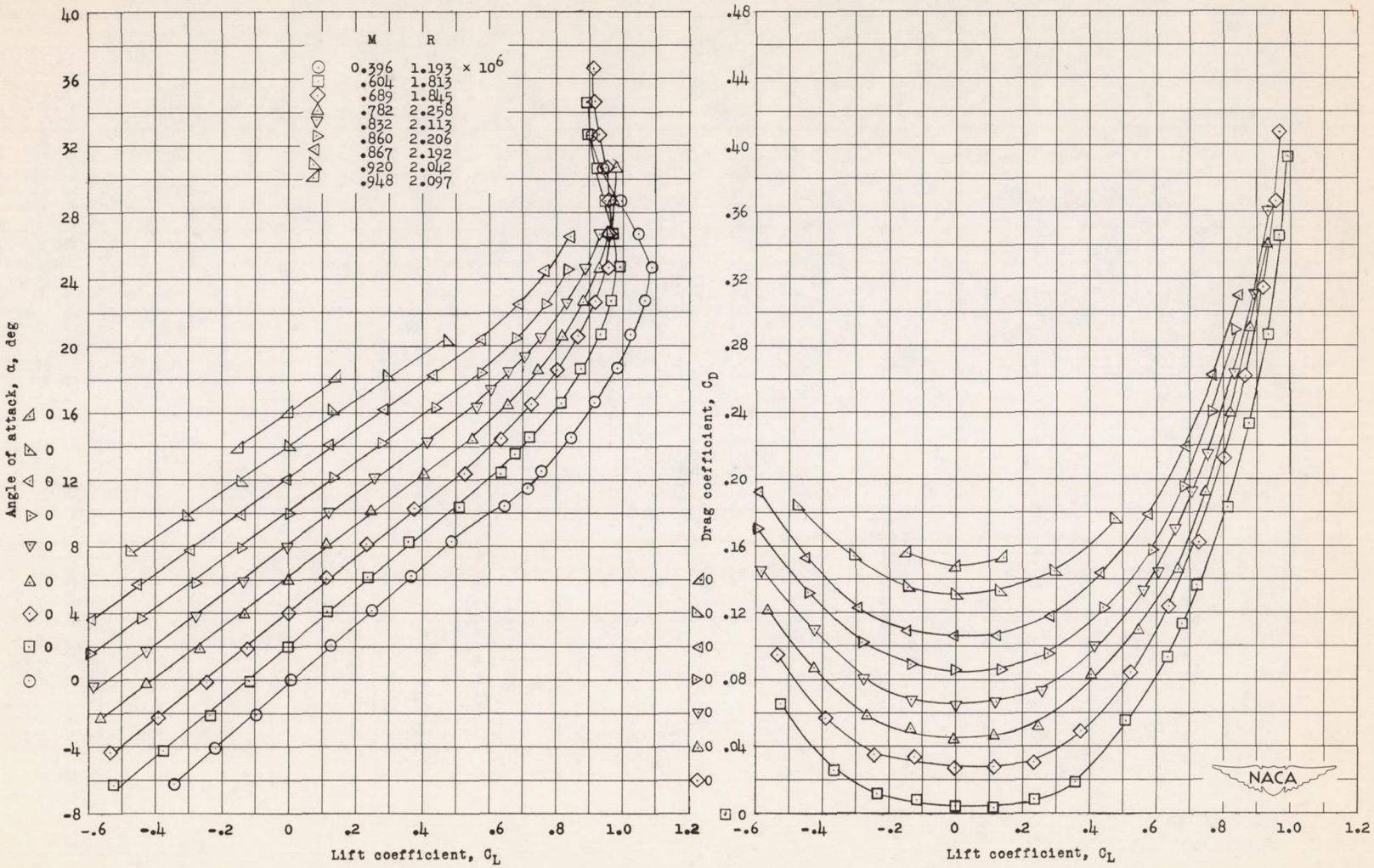


(a) Stagnation pressure, 6 inches of mercury.

Figure 11.- High-speed aerodynamic characteristics of the plain wing in a smooth condition at various Reynolds numbers and Mach numbers. NACA 2-006 airfoil section.

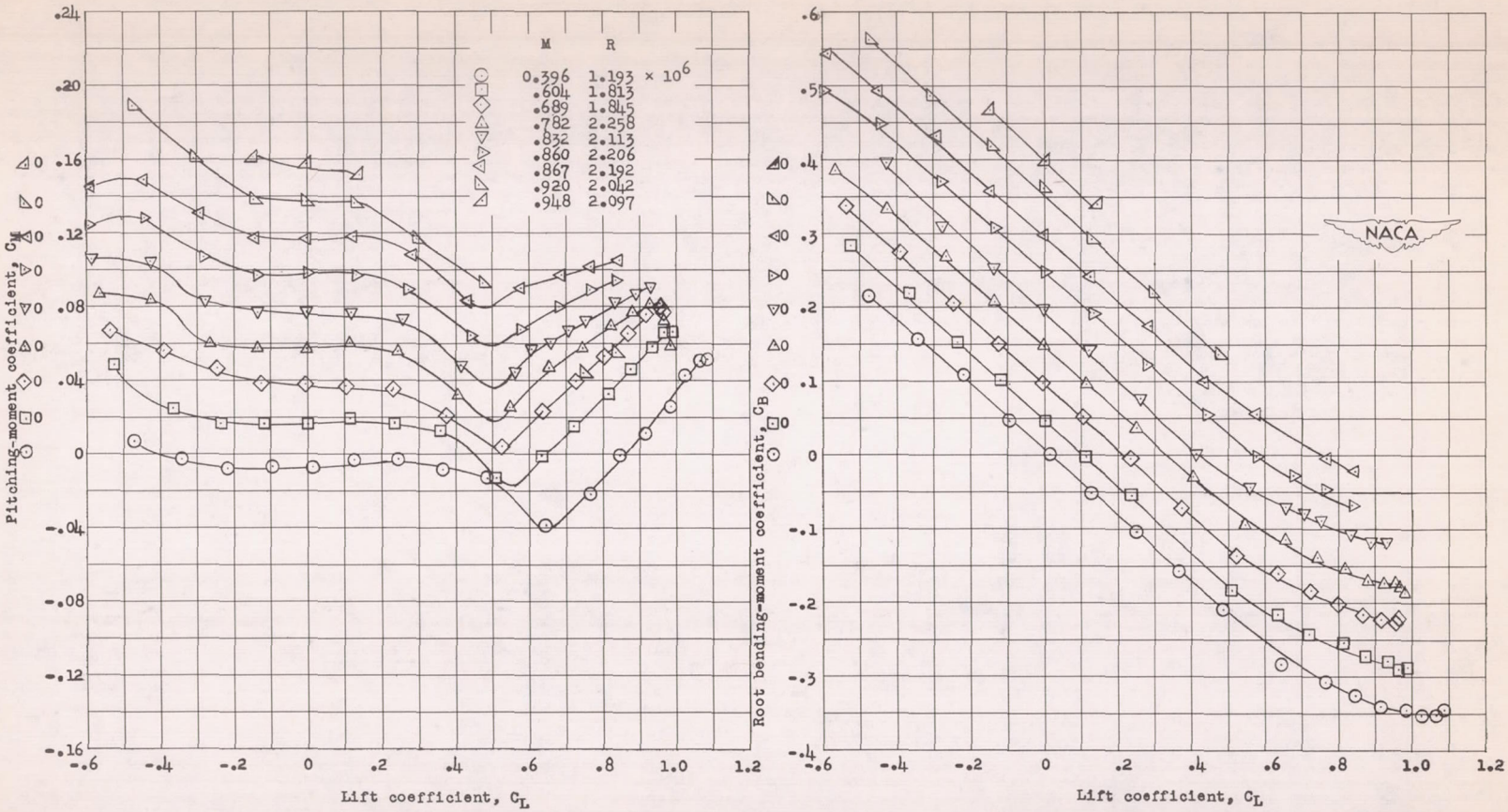


(a) Concluded.

Figure 11.- Continued.

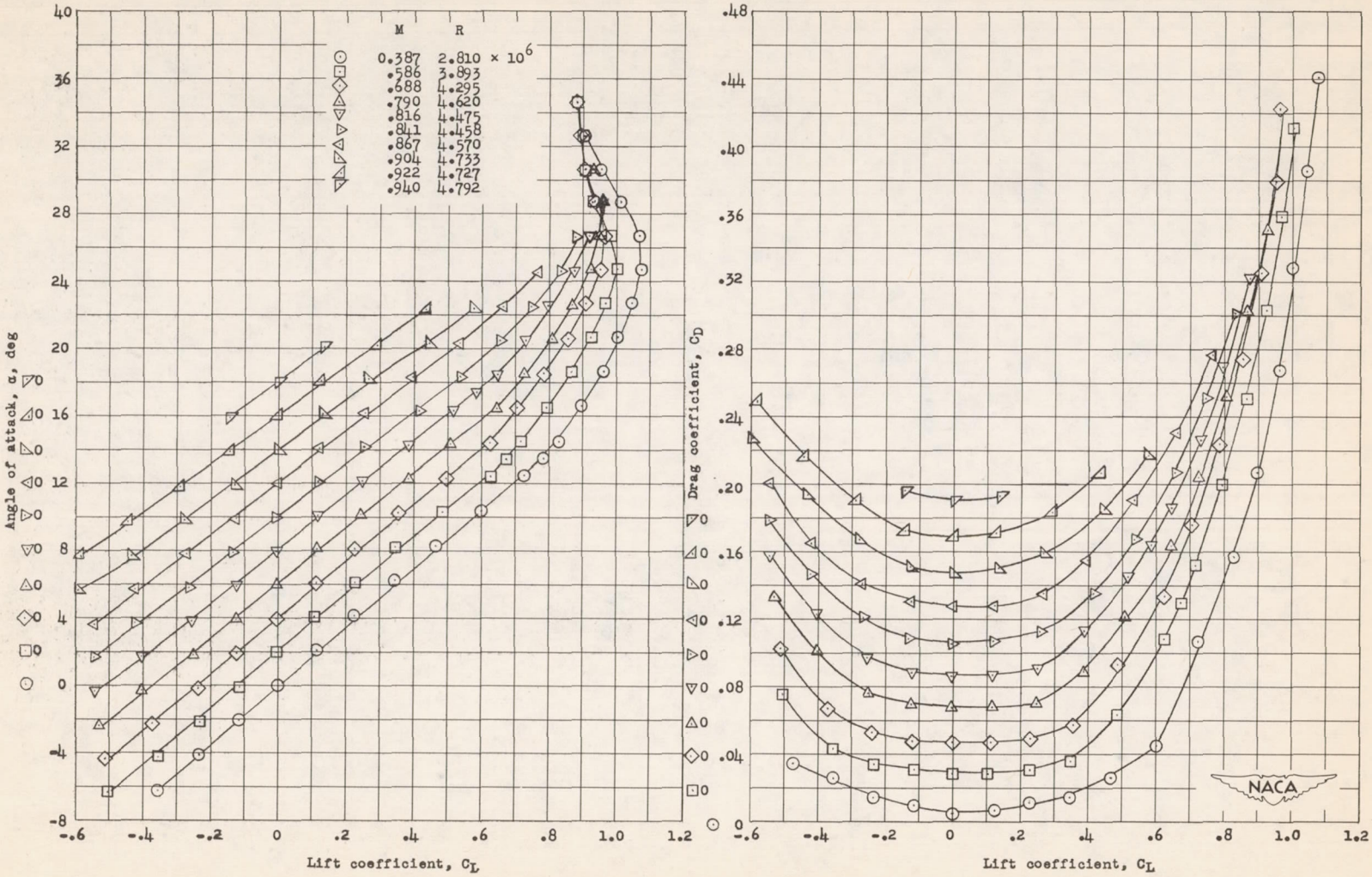


(b) Stagnation pressure, 15 inches of mercury.

Figure 11.- Continued.

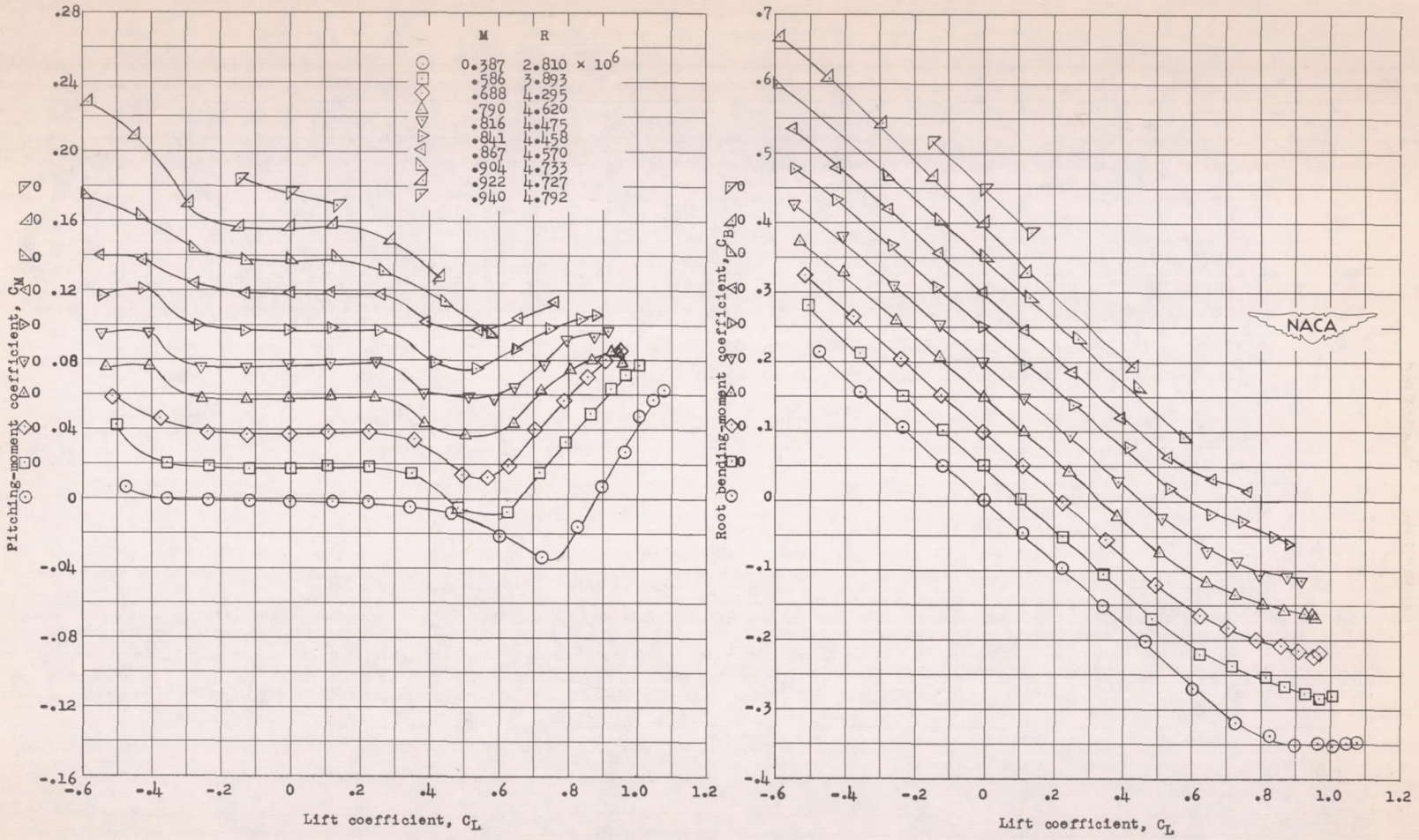


(b) Concluded.

Figure 11.- Continued.

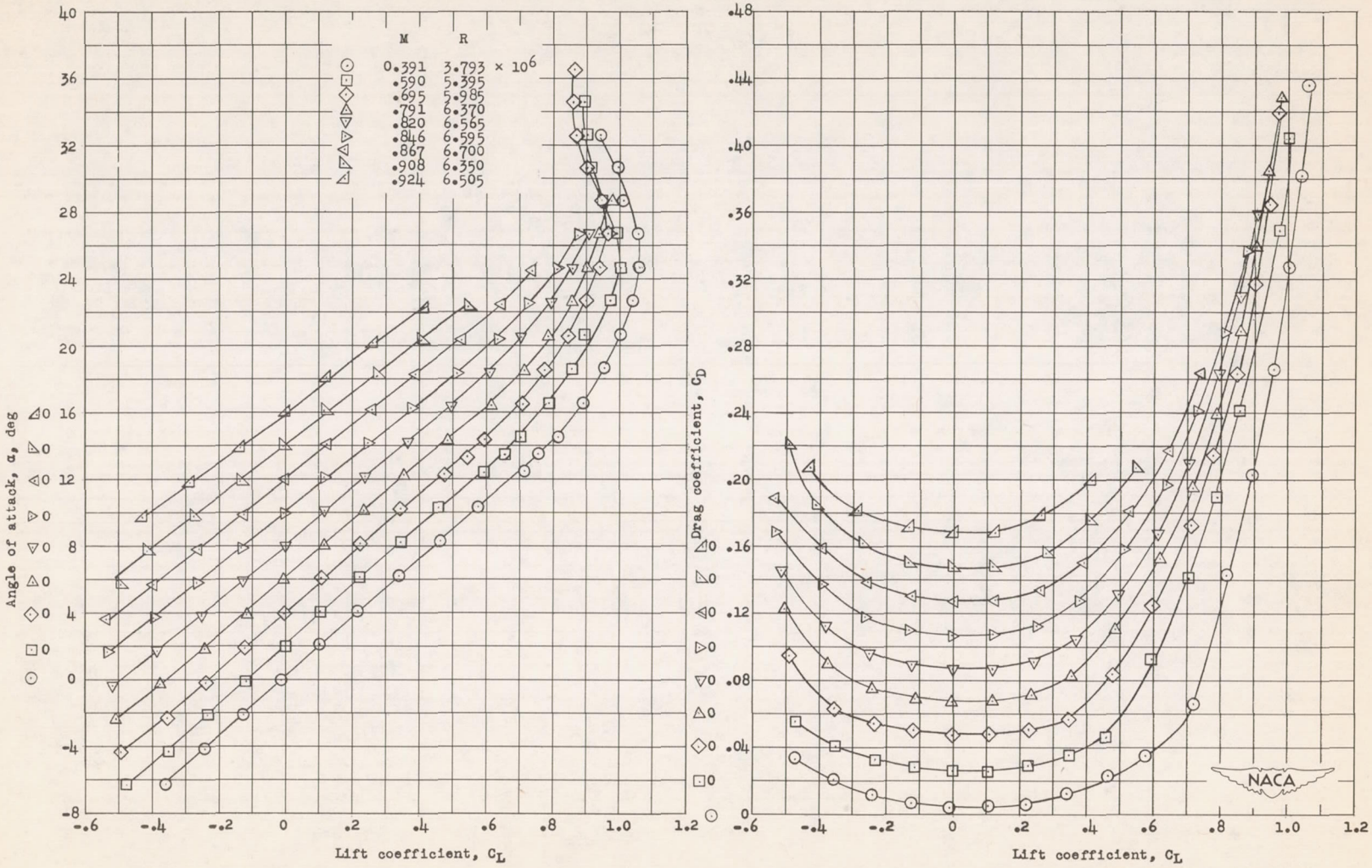


(c) Stagnation pressure, 20 inches of mercury.

Figure 11.- Continued.

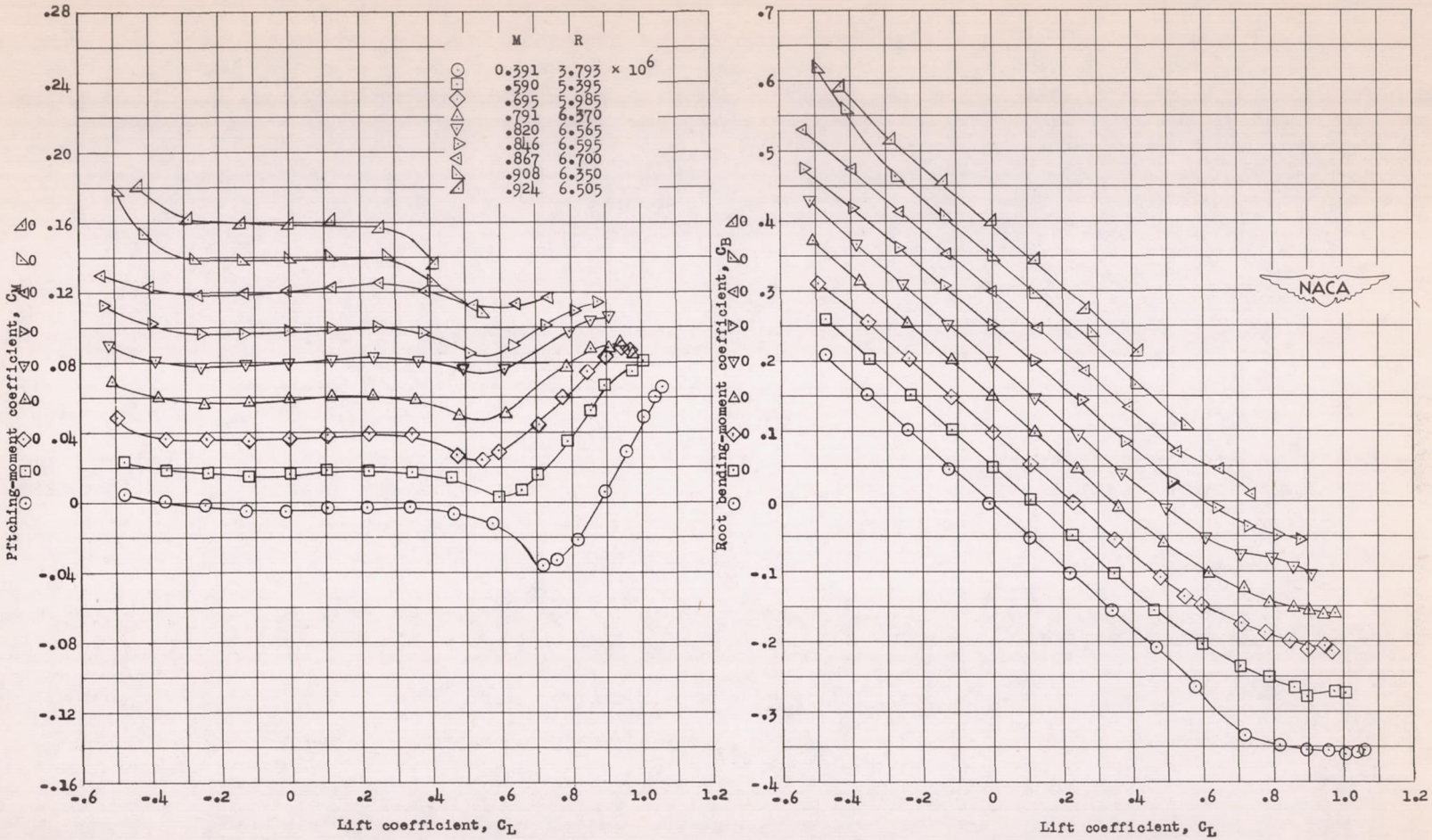


(c) Concluded.

Figure 11.- Continued.

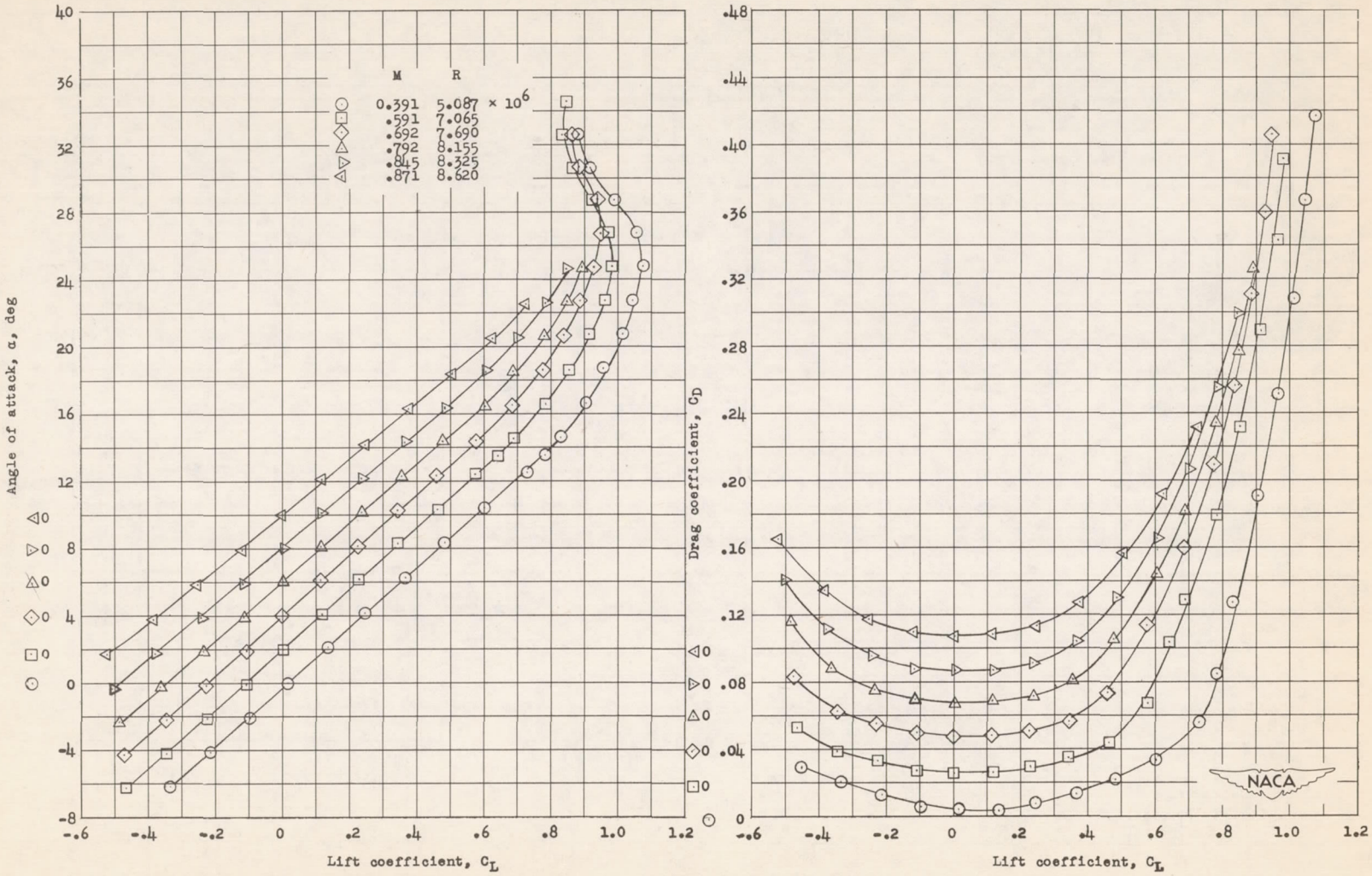


(d) Stagnation pressure, 27 inches of mercury.

Figure 11.- Continued.

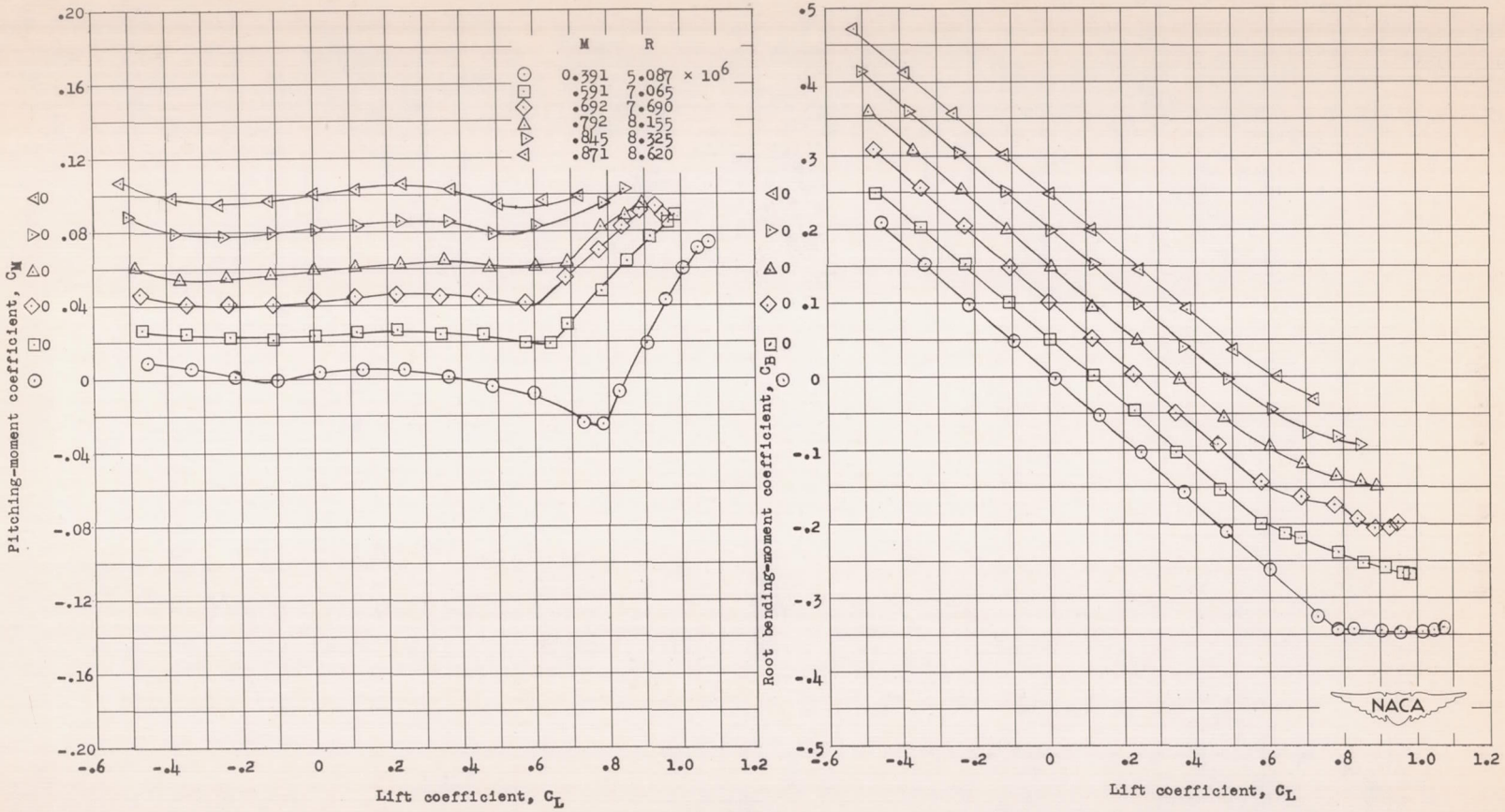


(d) Concluded.

Figure 11.- Concluded.

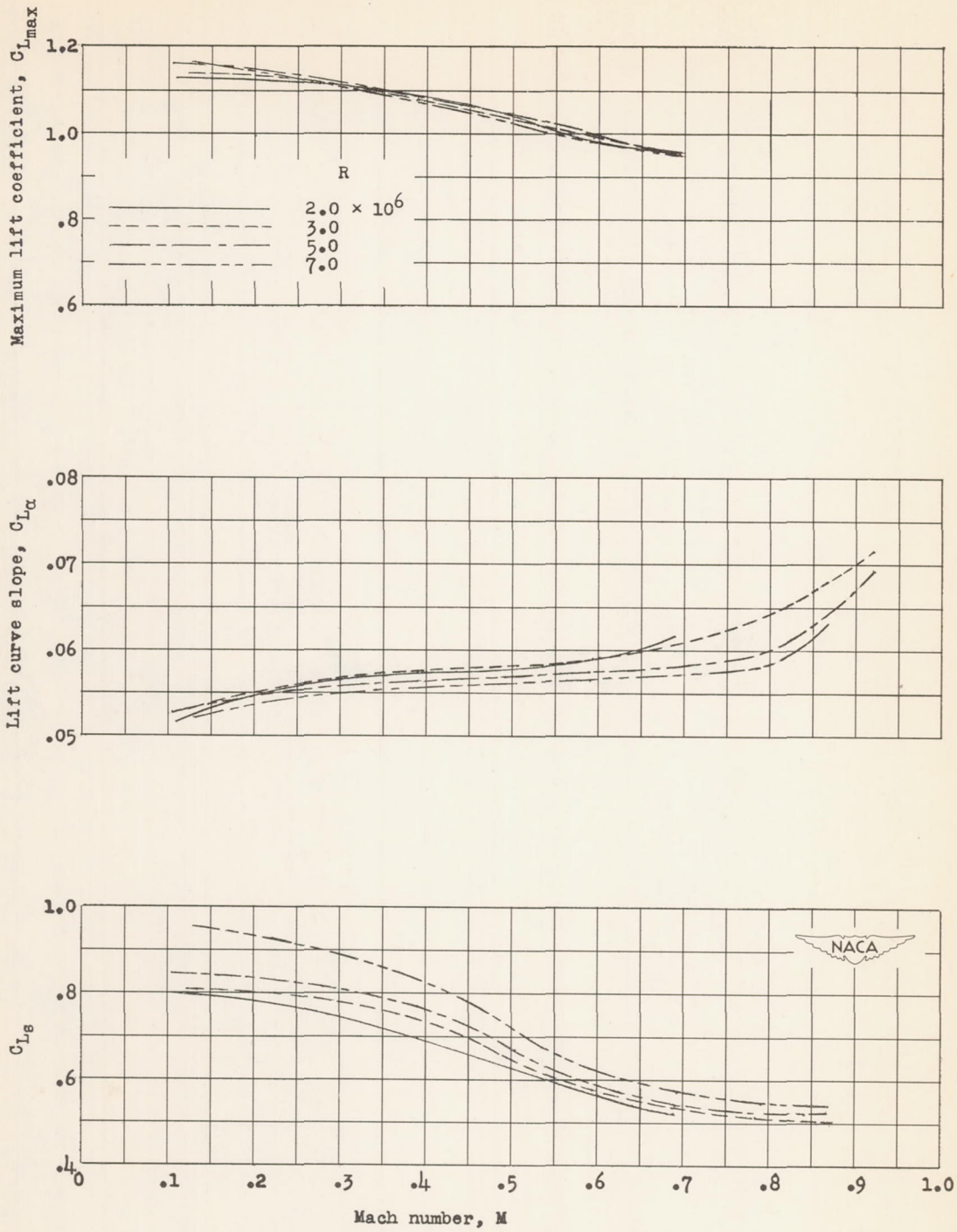


(a) Lift and pitching-moment characteristics.

Figure 12.- Aerodynamic characteristics of the wing with an NACA 2-006 airfoil section for various Reynolds numbers; model in smooth-surface condition.

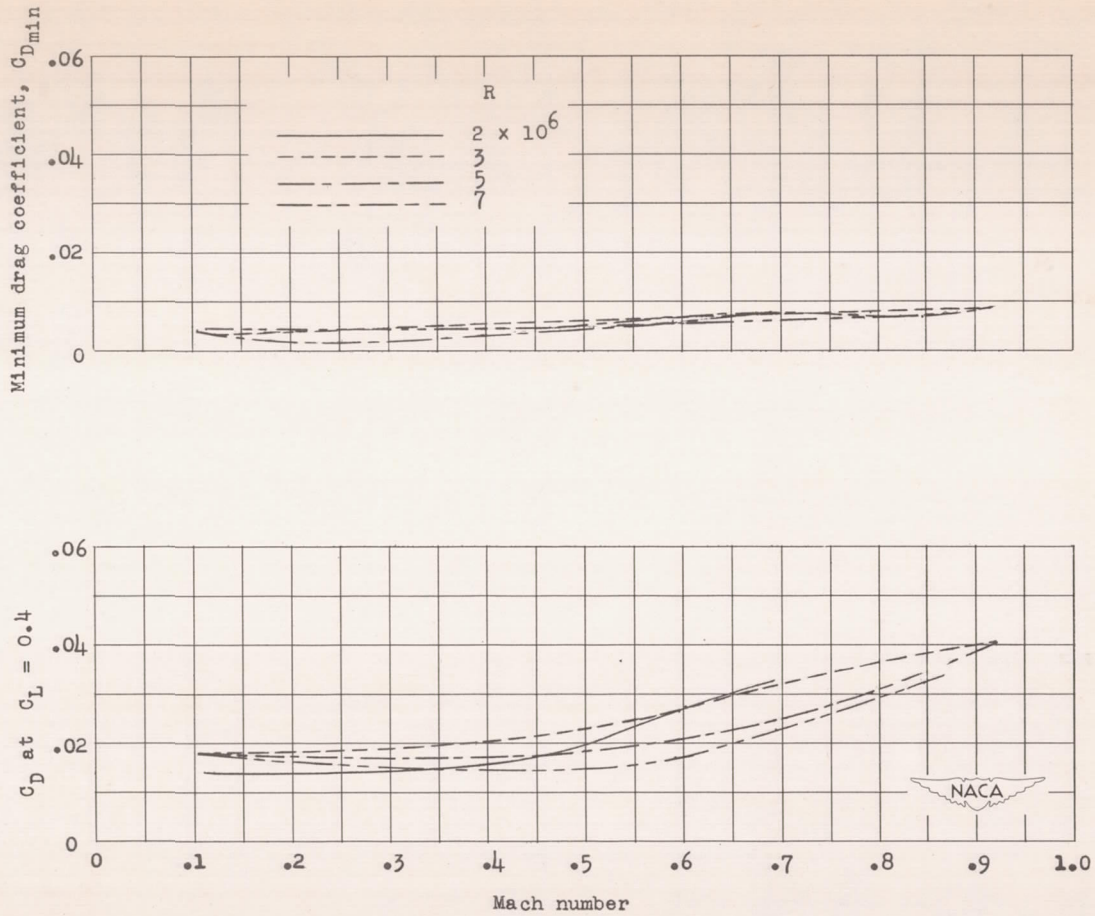


(b) Drag characteristics.

Figure 12.- Concluded.

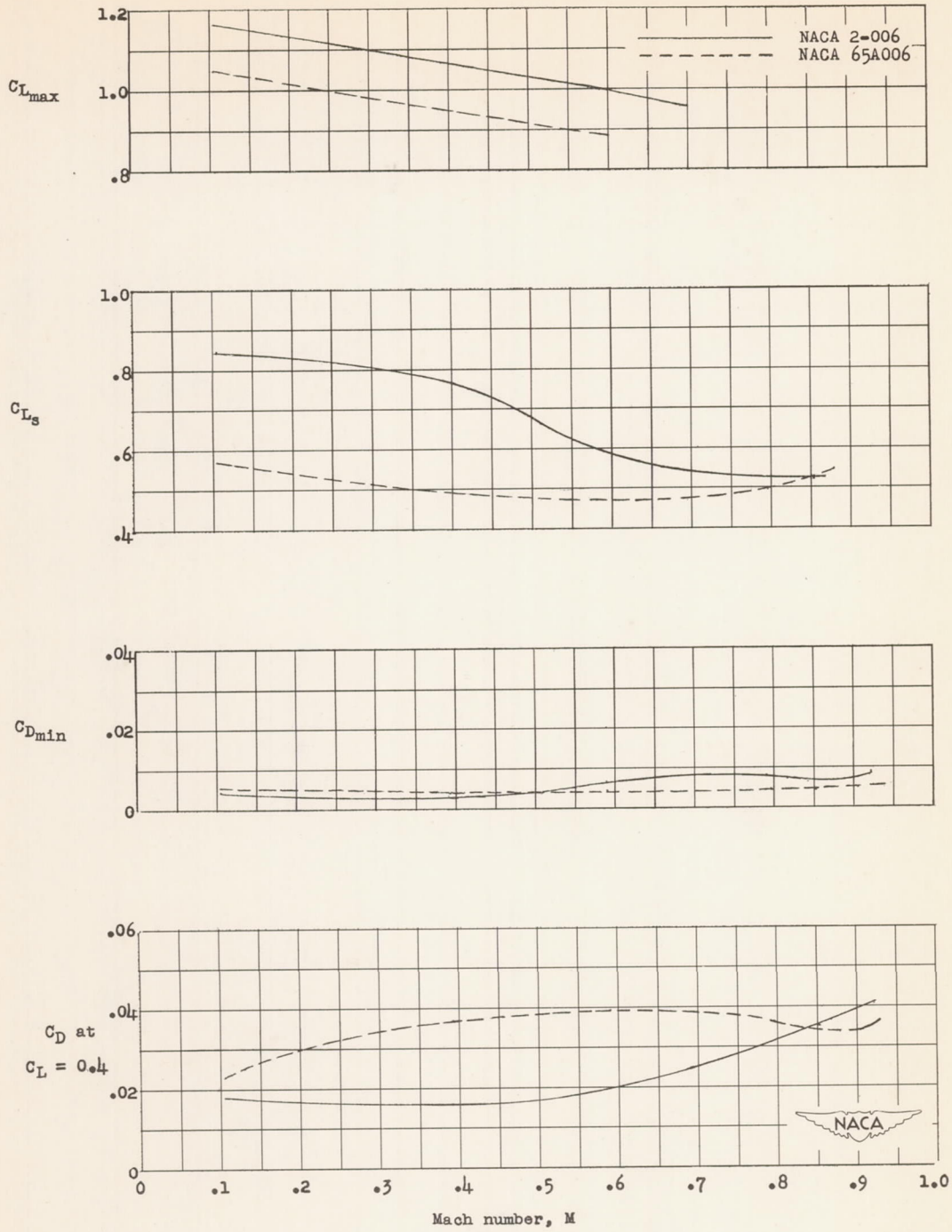


Figure 13.- Comparison of the aerodynamic characteristics of two wings of similar plan form with the NACA 2-006 and NACA 65A006 airfoil sections. Smooth-surface condition; $R = 5.0 \times 10^6$.

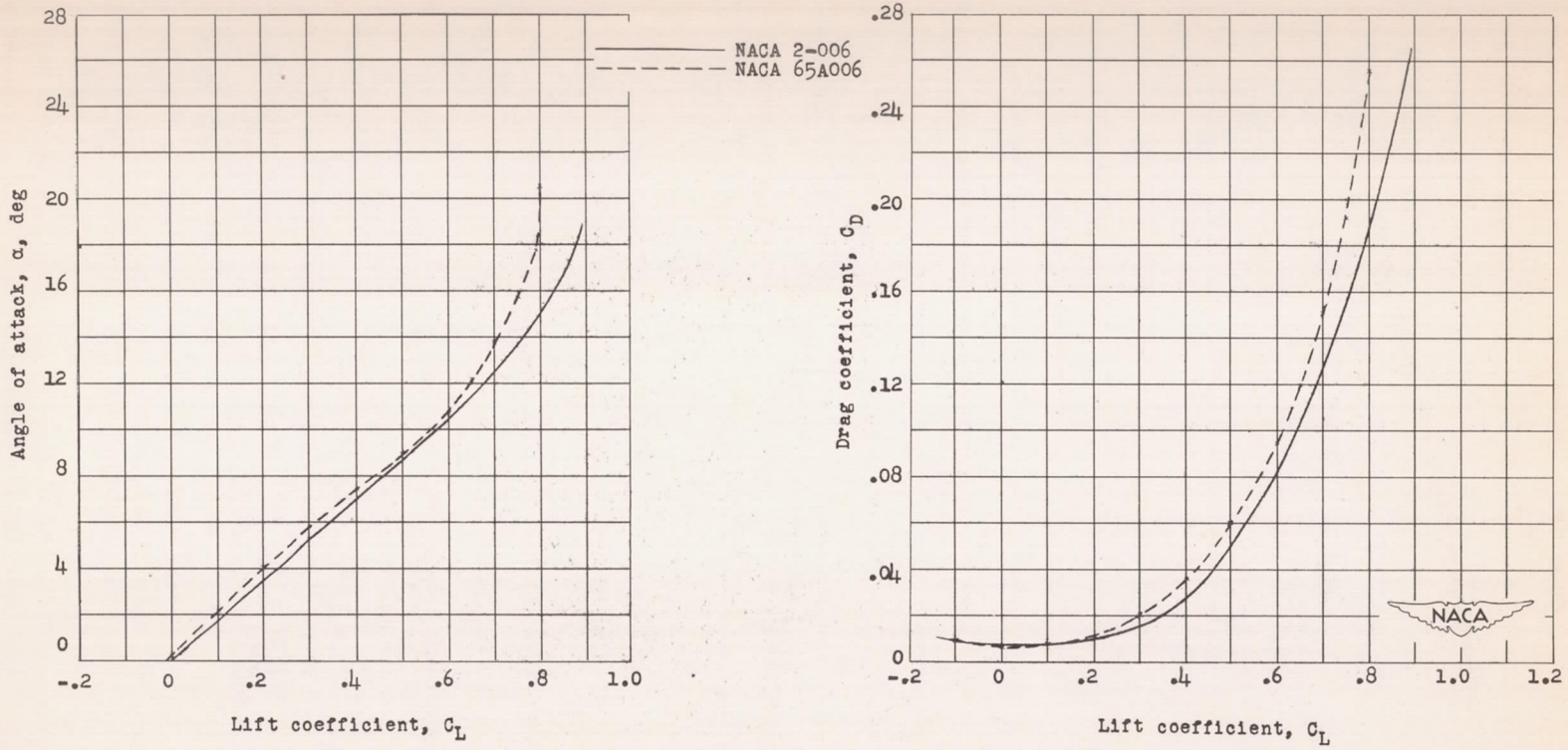


(a) Angle of attack and drag.

Figure 14.- Comparison of the high-speed aerodynamic characteristics of two wings of similar plan form with the NACA 2-006 and NACA 65A006 airfoil sections. Smooth-surface condition; M = 0.79; R = $8.2 \times 10^6$.

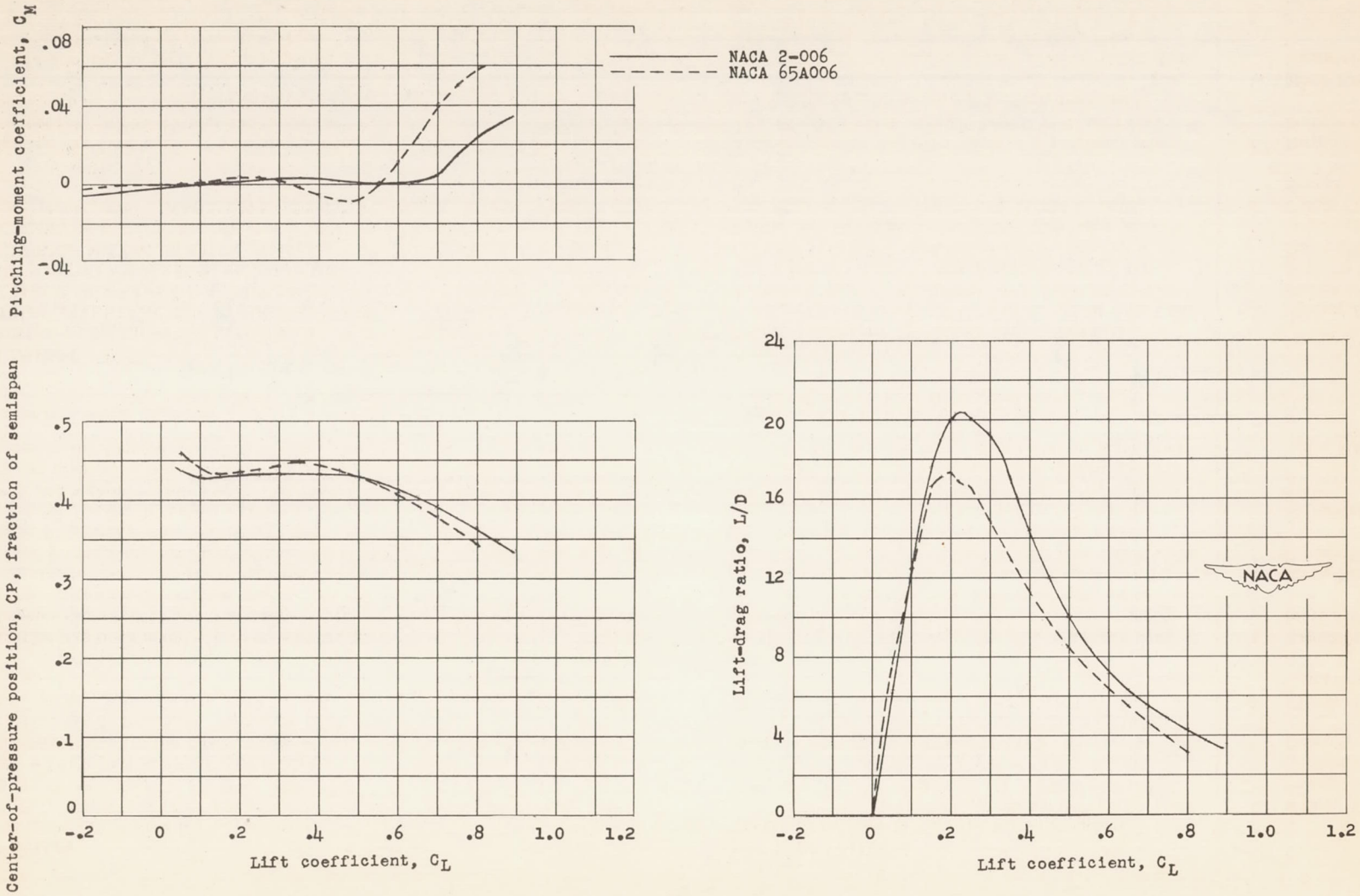


(b) Pitching moment, center of pressure, and lift-drag ratio.

Figure 14.- Concluded.